Volume 86, Number 8 August 2016

Journal of Sedimentary Research

An International Journal of SEPM
(Society for Sedimentary Geology)

Journal of Sedimentary Research

Journal of Sedimentary Research, 2016, v. 86, 944–964
Research Article
DOI: http://dx.doi.org/10.2110/jsr.2016.60

AN ABANDONED-CHANNEL FILL WITH EXQUISITELY PRESERVED PLANTS IN REDBEDS OF THE CLEAR FORK FORMATION, TEXAS, USA: AN EARLY PERMIAN WATER-DEPENDENT HABITAT ON THE ARID PLAINS OF PANGEA

SHARANE S.T. SIMON,[1] MARTIN R. GIBLING,[1] WILLIAM A. DiMICHELE,[2] DAN S. CHANEY,[2] CINDY V. LOOY,[3] AND NEIL J. TABOR[4]
[1]*Department of Earth Sciences, Dalhousie University, Halifax, Nova Scotia B3H 4R2, Canada*
[2]*Department of Paleobiology, National Museum of Natural History, Smithsonian Institution, Washington, D.C., 20013-7012, U.S.A.*
[3]*Department of Integrative Biology and Museum of Paleontology, University of California, Berkeley, California 94720, U.S.A.*
[4]*Department of Geological Sciences, Southern Methodist University, Dallas, Texas 75275, U.S.A.*
e-mail: sharane.simon@dal.ca

ABSTRACT: **A well preserved plant assemblage at the Colwell Creek Pond locality of Leonardian (Kungurian) age provides an opportunity to evaluate taphonomic conditions in a dryland alluvial setting. A narrow channel body incised to 5 m depth through red paleo-Vertisols contains 2 m of varicolored laminated mudstone with graded layers and plant material. X-ray diffraction analysis of individual laminae indicates the presence of chlorite, illite, kaolinite, and mixed-layer clay, with hematite in red and gray layers and goethite in yellow-brown laminae. No carbonate was identified, and the total organic carbon content is minimal. The fine sediment accumulated in a shallow abandoned channel from suspension and gentle underflows, probably linked to seasonal inflow, and analysis of lamina thickness suggests that standing water may have persisted for up to a few millennia. The preservation of lamination is attributed to a lack of bioturbation, possibly linked to a paucity of subsurface oxygen, low productivity, elevated salinity, rapid deposition, or a combination of these factors; minimal bioturbation may also reflect the limited use of freshwater ecospace during the Early Permian. Clay-rich paleo-Vertisols complete the fill, with drab root traces that indicate growth of vegetation in a strongly seasonal setting.**

Abundant plant material in the laminated beds includes branches of walchian conifers, the possible cycadophyte *Taeniopteris* spp., and the comioid, possible peltasperm, *Auritifolia waggoneri*. They were derived from an adjacent riparian zone and preserved as 3D goethite petrifactions. Much of the foliage shows evidence of arthropod herbivory. Although a humid climatic episode cannot be ruled out, the exceptional abundance and preservation of the plants probably reflects the persistence of an oxbow lake on a relatively arid alluvial plain, where riparian plants experienced periodic moisture stress but had access to groundwater nearly year round. Rapid burial in standing water, the lack of bioturbation in the laminated sediments, and early biomineralization probably explain the exceptional preservation of the plant remains.

INTRODUCTION

As the supercontinent Pangea assembled through the Late Pennsylvanian and Permian, alluvial plains across Euramerica experienced progressive aridification, with thick loess accumulations and arid paleosols (Kessler et al. 2001; Tabor and Poulsen 2008; Tabor 2013). Based on the analysis of fluid inclusions in halite, estimated surface temperatures were at times as extreme as in any place on Earth today (Zambito and Benison 2013). Floral assemblages across western Euramerica changed in step with this climatic evolution (DiMichele and Aronson 1992; Rees et al. 2002; DiMichele et al. 2006; Montañez et al. 2007).

Surprisingly in view of this aridity, well-exposed Pennsylvanian and Permian alluvial formations across north-central Texas have yielded rich assemblages of exquisitely preserved plant fossils and a diverse range of vertebrates (Olson 1958; Olson and Bolles 1975; Olson and Mead 1982; Murry and Johnson 1987; Olson 1989; DiMichele et al. 2006; Chaney and DiMichele 2007; Chaney et al. 2009; Mamay et al. 2009; Tabor et al. 2013). Rare occurrences of plant fossils have been recorded in upper Permian and Triassic redbeds elsewhere, where plant remains were commonly preserved in gray lenses and within laminated sediments in lakes and abandoned channels (Demko 1995; Clausing and Boy 2000; Galtier and Broutin 2008; Bercovici et al. 2009). Hypotheses to explain these occurrences include 1) periodically humid and well vegetated conditions that reflect climatic change, 2) local groundwater-dependent habitats in an otherwise dry landscape, 3) plant preservation under unusual taphonomic conditions, or 4) a combination of these factors (DiMichele et al. 2006; Montañez et al. 2007; Looy 2013).

In the Clear Fork Formation of Texas, a prominent floral site is Colwell Creek Pond, interpreted as an oxbow lake (Chaney et al. 2009; Looy 2013; Schachat et al. 2014). Excavated periodically over 20 years, the site is the most heavily collected plant-bearing locality from a single depositional environment in the Leonardian redbed section of north-central Texas. The flora was briefly discussed by Schachat et al. (2014) in the course of their characterization of insect damage on the plants.

Published Online: August 2016
 1527-1404/16/086-944/$03.00

The plant fossils are preserved in thinly laminated beds with subtle layer-by-layer color variation, for which no sedimentological or technical analysis was previously available. Although abandoned-channel fills worldwide commonly contain laminated intervals, such thinly laminated beds constitute a rarely documented facies that is prominent at numerous localities in the Clear Fork Formation. Plant fossils are present at many of these sites, and understanding the nature and origin of the laminated beds at Colwell Creek Pond is central to an assessment of plant preservation in this unusual facies. The present study documents 1) the facies and geometry of the alluvial strata, 2) the sedimentary structures, mineralogical composition, and organic content of the laminated beds, 3) the main plant taxa, and 4) the characteristics of the associated paleosols. We conclude that the locality represents a local well-watered habitat in a relatively arid landscape, where water influx to the channel offset a high rate of evapotranspiration. A well vegetated channel margin supplied leaves and branches to standing water where favorable taphonomic conditions included early biomineralization.

GEOLOGIC SETTING

The Clear Fork Formation was deposited on the Eastern Shelf of the Midland Basin, which lay between 0° and 5° N of the equator across the western coastal zone of Pangea during the late Paleozoic (Fig. 1A; Ziegler et al. 1997). The Wichita, Arbuckle, and Ouachita Mountains to the east rose during the Pennsylvanian, but Early Permian tectonic activity was limited to intermittent strike-slip movements along the Matador–Red River uplifts (Regan and Murphy 1986a; Budnik 1989; Brister et al. 2002). During the Permian, clastic sediments were sourced mainly from recycled Pennsylvanian fan deltas and fluvial facies, reflecting substantial denudation of the uplifts (Brown 1973; Hentz 1988; Tabor and Montañez 2004). The formation is near horizontal with a gentle WNW dip ($< 1°$) but with little other evidence of deformation (Edwards et al. 1983; Hentz 1988).

The Clear Fork Formation rests conformably on dolostone and mudstone beds of the Lueders Formation, which is interpreted as a tidal deposit based collectively on an assemblage of brackish-water invertebrates, plants, and tetrapods with channel deposits that intercalate or correlate with carbonate rocks containing marine invertebrates (DiMichele et al. 2006). In north-central Texas, the Clear Fork Formation comprises 350–365 m of terrestrial deposits, mainly red mudstone with minor sandstone, carbonates, and evaporites (Fig. 1B; Olson 1958; Nelson et al. 2013). In this area, Nelson et al. (2013) subdivided the formation into informal lower, middle, and upper units, with the Colwell Creek Pond site in the middle unit. The paleoenvironment northwest of Seymour has been interpreted as continental on the basis of sedimentology and biota, with possible marine influence in the basal strata (Olson 1958; Murry and Johnson 1987; DiMichele et al. 2006) and playa-lake deposits at a locality to the southwest (Minter et al. 2007). Fine-grained meandering-channel and floodplain deposits are prominent, with plants, vertebrates, and tetrapod and myriapod trackways and paleoflow to the southwest (Olson 1958; Edwards et al. 1983; Lucas et al. 2011; Nelson et al. 2013). Pedogenic carbonate and gypsum nodules are present, the latter increasing in prominence upwards (DiMichele et al. 2006). Approximately 200 km to the south, open-marine intervals with limestone and dolomite are present at equivalent levels (Olson 1958, 1989; Olson and Mead 1982; Nelson et al. 2013). Although marine influence cannot be discounted for the low-gradient plain of the study area, no evidence currently supports such an interpretation at the level of the Colwell Creek Pond site. Conformably overlying the Clear Fork is the San Angelo Formation of the Pease River Group, laid down in multi-channel systems and suspended-load meandering rivers (DiMichele et al. 2006).

The burial history of the Eastern Shelf is not well documented, but the maximum burial depth of the Virgilian strata, less than 500 m below the Clear Fork Formation, may not have exceeded 1600 m (Tabor and Montañez 2004). Virgilian coals and carbonaceous shales have low R_o values of 0.4–0.8% (Hackley et al. 2009), and burial temperatures of less than 40–45°C were estimated from Early Permian strata along the flanks of the Midland Basin (Bein and Land 1983; Tabor and Montañez 2004). These data collectively suggest that the Clear Fork Formation experienced shallow burial and a low degree of thermal maturation, implying only modest diagenetic change in clays and other minerals during burial.

METHODS

The outcrops at Colwell Creek Pond, which derives its name from a nearby creek draining into the North Fork of the Wichita River, are exposed along cliffs (10 m high), partially covered by a weathered layer and sparse vegetation (Fig. 2). Located in Knox County, the exposures extend for 60 m across 0.85 hectares and are oriented northeast to southwest. Lithology, grain size, and sedimentary features were recorded, leading to the identification of seven lithofacies (Table 1). Two profiles were measured and combined to create a composite section divided into channel bodies 1 and 2, in upward succession (Fig. 3A). A profile was measured in a floodplain section under the margin of Channel Body 1 (Fig. 3B).

To reconstruct the orientation and geometry of Channel Body 1, the strike and dip of the beds were recorded with GPS locations accurate to ± 3 m. Paleoflow readings were measured from rib and furrow structures on ripple cross-laminated beds to an accuracy of ± 5°. Location coordinates were used to map the basal surface of the channel body in ArcGIS (Fig. 4). Using photomontages of the cliffs, the distance above the channel base was determined with a precision of ± 0.1 m. For points measured away from the cliffs where photomontages were unavailable, the height of each point above the channel base was obtained from a Google Earth elevation profile with a precision of ± 0.3 m. A cross section was generated by projecting data points of known elevations onto a line perpendicular to the mapped channel margin (line A–A′; Fig. 4). A best-fit curve was generated, broadly defining the base of the channel body.

The laminated beds containing the plant fossils were studied for lamina thickness and geometry and for sedimentary structures (Figs. 5, 6), and three unpolished thin sections were studied under plane-polarized light (Figs. 7A, B). Thickness measurements were acquired from thin sections rather than block samples because the layers contain sub-laminae that could not be distinguished in hand specimens. Furthermore, the layers pinch out laterally within a few centimeters in block samples and are commonly contorted, whereas thin sections provide a narrow, high-resolution cut through the layers, aiding precise thickness measurement. Due to the delicate nature of the rocks, large mudstone slabs were not collected in the field, which precluded analysis of trends in lamina characteristics. A polished thin section studied using a LEO 1450 VP Scanning Electron Microscope with an INCA X-max 80 mm 2 EDS system provided semiquantitative elemental information. Because mineral grains are smaller than the analyzed spot size of 10 μm, the results yield only a general guide to the minerals present. The thin section was polished with a lead block, and embedded lead fragments were recorded as artefacts. The backscatter images were used to determine grain size and composition and to highlight textural variations (Figs. 7C–F).

X-ray diffraction (XRD) analysis was conducted at Bedford Institute of Oceanography on nine randomly oriented powder mounts of individual laminae with varied color (Fig. 8A). The surfaces of laminae were exposed using a hammer and a metallic file, and material was removed using a thin blade, with the first scraping avoided to reduce contamination. The samples were crushed using a mortar and pestle, and powder colors were estimated using a Munsell Geological Rock Color Chart. XRD was carried out with a Siemens Kristaloflex diffractometer using Co-Kα radiation.

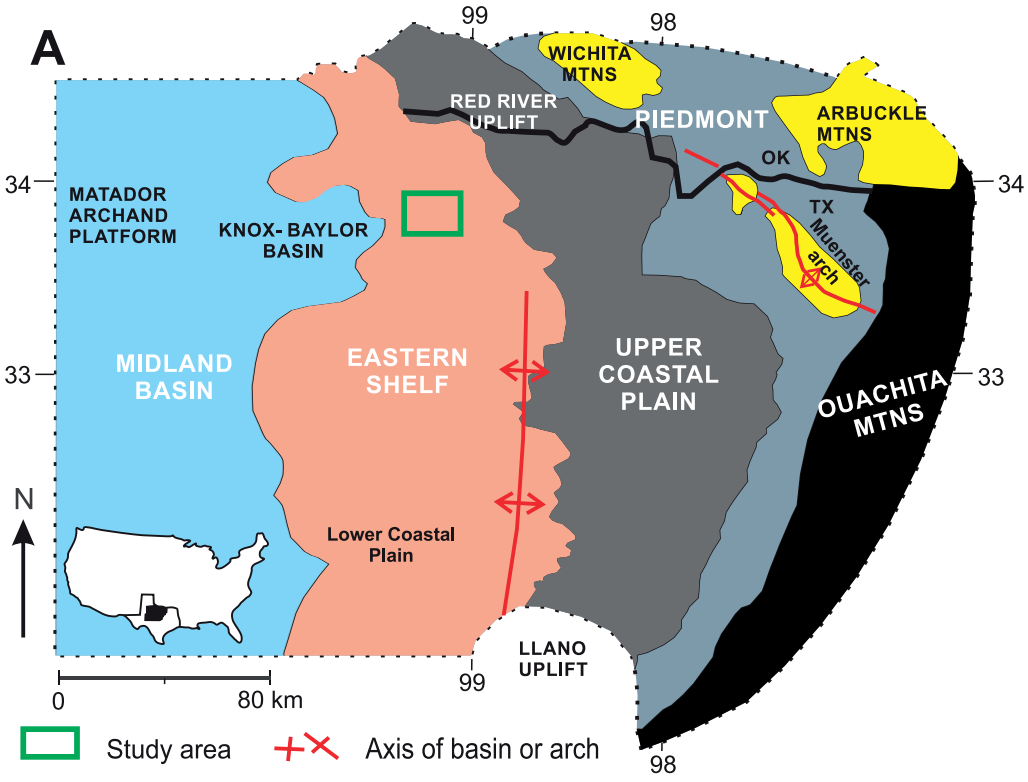

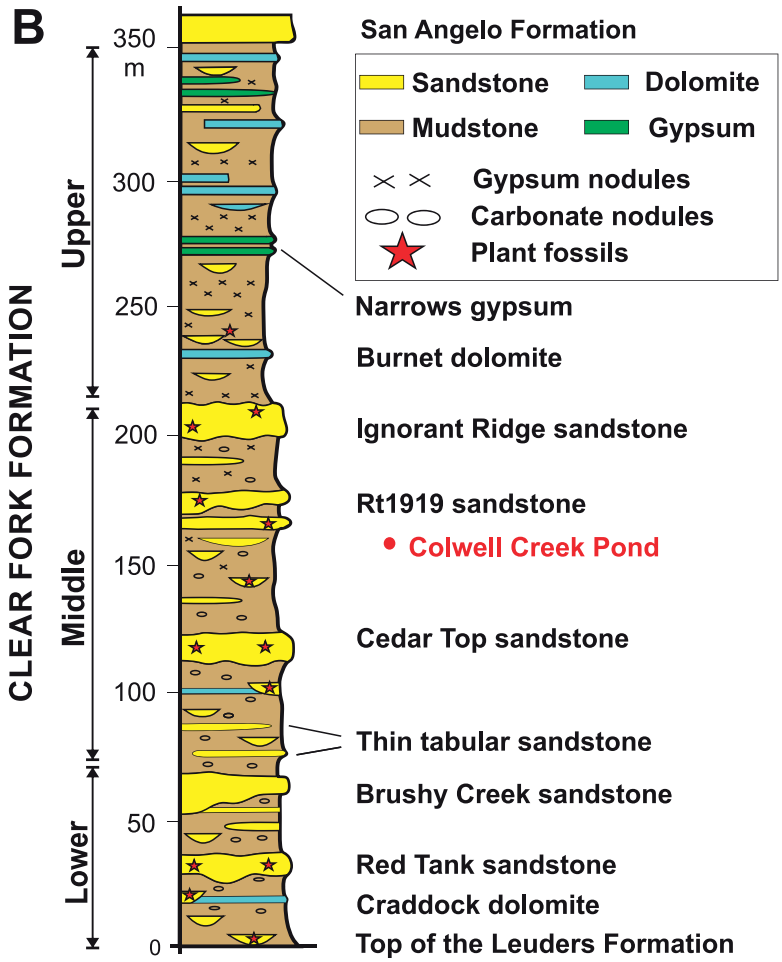

FIG. 1.—**A)** Pennsylvanian–Permian paleogeography of the eastern part of the Midland Basin, highlighting the main uplifts and basin areas (modified from Tabor and Montañez 2004). The green box marks the Clear Fork Formation study area. **B)** Composite log of the Clear Fork Formation along the Wichita River, showing the occurrence and relative thicknesses of the main channel bodies (modified from Nelson et al. 2013). The Colwell Creek Pond site is located in the middle unit of the Clear Fork Formation.

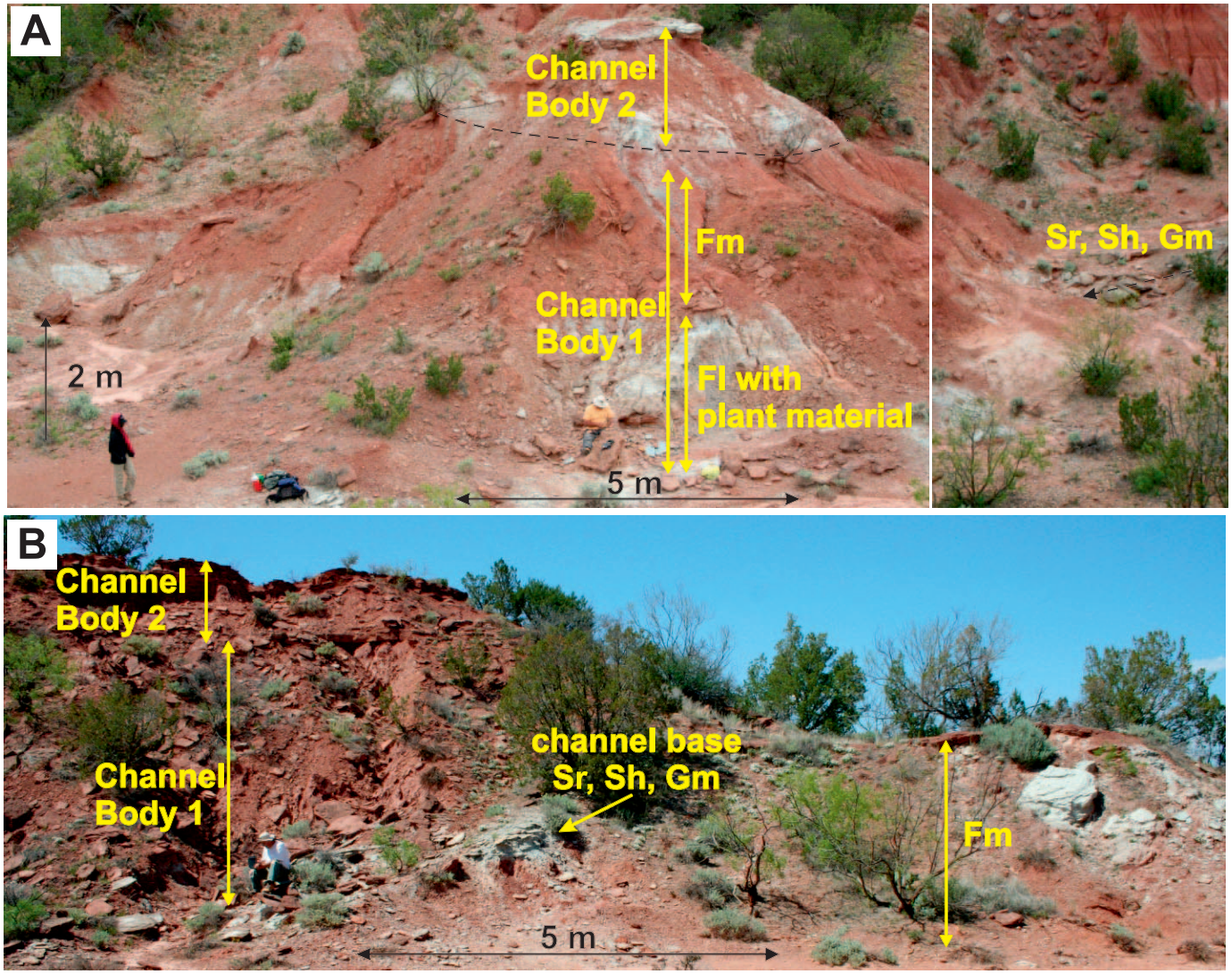

FIG. 2.—Outcrops at Colwell Creek Pond. Yellow arrows denote the positions of detailed lithological logs. **A)** Main cliff section 7 m high, subdivided into Channel Bodies 1 and 2. The lower stratigraphic interval is subdivided into lithofacies shown in Table 1 (Fm, massive mudstone; Fl, laminated mudstone; Sr, ripple cross-laminated sandstone; Sh, planar-stratified sandstone; and Gm, massive pebbly conglomerate). **B)** Adjacent cliff section highlighting the contact of the two channel bodies and that of the lower channel body with underlying floodplain deposits (Fm). The cliff lies parallel to and 20 m northwest of the main cliff section.

Bulk slides were scanned from 2° to 77° 2θ, with a 0.2° step interval and 2 s step time.

Two samples were selected for a <2 μm fraction analysis. Approximately 20 g of crushed sample was suspended in a burette containing a weak solution of sodium hexametaphosphate. After 16 hours, the < 2 μm fraction was isolated, flocculated with 4 ml of $MgCl_2$ solution, and centrifuged. The mixture was decanted and the clay fraction was resuspended in a 500 ml cylinder. A 20 ml aliquot was withdrawn, dried, and weighed to determine the appropriate weight (5%) for the internal standard, zincite. The zincite was added to the resuspended sample and dissolved using a laboratory shaker, after which the sample was centrifuged and smeared on a normal glass slide and a second heat-resistant glass. Using the scan properties described above, XRD analysis for the < 2 μm fraction was carried out using the normal glass slides. The slides were then placed in a desiccator containing vapors of ethylene glycol for ~ 4 hours to investigate peak shifts, after which they were analyzed immediately to prevent the glycol from evaporating, using a 2–17° 2θ range with a 0.2° step interval and 2 s step time. The heat-resistant slides were placed in a preheated furnace at 150°C for at least 30 minutes, and were analyzed using a 2–30° 2θ range with a 0.2° step interval. This process was repeated for 300°C, 500°C, and 650°C, which allowed clay minerals to be identified by revealing changes in crystal structure spacing (Fig. 8B). At temperatures > 500°C, most clay smears started to flake or bubble, and XRD analysis was not conducted on these samples.

For three samples from the floodplain interval, oriented aggregates were treated to produce potassium- and magnesium-saturated mounts, with and without glycerol solvation, and analyzed at Southern Methodist University using a Rigaku Ultima III X-ray diffractometer with Cu-Kα radiation from 2° to 30° 2θ with a 0.05° step interval per s. The potassium-saturated samples were heated in a furnace at 500°C for at least two hours. Mineral identification of the laminated beds and floodplain deposits followed Moore and Reynolds (1997) and the JCPDS (Joint Committee on Powder Diffraction Standards) Powder Diffraction File system. Components of mixed-clay layers were not identified, and no attempt was made to quantify clay-mineral proportions, although general comparisons were possible using peak intensities.

TABLE 1.—*Lithofacies in the Colwell Creek Pond outcrops, using terminology from Miall (1985, 1996), Tucker (2003), and Long (2011). VF, F, M, and VC, very fine, fine, medium, and very coarse grains, respectively.*

Facies code	Lithofacies description	Sedimentary structures	Unit contacts	Fossils	Interpretation
Fl	Variegated, laminated mudstone	Lamination, cross lamination, graded bedding, loop bedding and microfaults, soft-sediment deformation, load casts, overturned beds, scours	Parallel-planar at base, to parallel to nonparallel wavy at top	Plant leaves and stems abundant	Suspension deposition from density underflows with minor compactional deformation
Fm	Brown, massive mudstone	Massive, locally weakly stratified, redoximorphic spots, slickensides	Poorly developed or irregular	Plant roots rare	Suspension deposition from standing water, with pedogenic overprinting. Paleosol development on the floodplains
Gm	Gray, massive pebbly conglomerate	Massive units of carbonate and mudstone clasts, locally weakly stratified and trough cross-stratified	Abrupt, planar or irregular, locally erosional	Vertebrate material rare	Channel lag associated with scouring events
Sl	Red, M sandstone, low-angle cross-stratified	Convex-up mound with form-concordant plane lamination	Sharp basal contact, gradational top	Not observed	Antidune formed under upper-flow-regime conditions
Sh	Red, VF to M sandstone, planar-stratified	Planar lamination	Undulating to planar contacts	Diplichnitid trackways abundant	Plane beds formed under upper-flow-regime conditions
St	Red, VC sandstone with minor granules, trough cross-bedded	Trough cross-beds, minor ripple cross-lamination	Sharp or erosional contacts	Plant stems rare	Accretion and migration of lower-flow-regime 3D dunes
Sr	Gray/red, VF to M, ripple cross-laminated sandstone	Ripple cross-laminated (non-climbing and slightly climbing), scours	Sharp, planar contacts	Not observed	Accretion and migration of current ripples under lower-flow-regime conditions

A split from each of the nine samples was ground and freeze-dried, and ~ 100 mg was analyzed for total carbon using a Leco TruSpec CHN (detection limit 0.01 wt. %). Another split was leached overnight with 10% HCl to remove inorganic carbon. A total of 100 mg of the leached sample was analyzed for organic carbon, and the inorganic-carbon content was calculated by difference (Table 2).

LITHOFACIES

Laminated Mudstone (Fl)

Description.—Laminated mudstone forms a single unit 203 cm thick that rests abruptly on coarser beds of facies Gm, Sr, and Sh in Channel Body 1. The laminae are predominantly red-brown with light brown, yellow, and gray layers (Table 2; Figs. 5B, 6). Grains of fine to coarse silt predominate as discrete layers and the coarser parts of graded beds.

Based on thin-section analysis of 34 laminae from three thin sections, the layers range from 0.2 mm to 2.1 mm thick, with an average of 0.7 ± 0.4 mm (1-sigma range). The gray and red-brown layers have a combined average thickness of 0.8 ± 0.5 mm, and the yellow laminae have an average thickness of 0.4 ± 0.1 mm. The lowermost laminae are thicker and slightly coarser grained (coarse silt). The gray and red-brown layers are difficult to discern in thin section, and no attempt was made to distinguish them (Fig. 7A). The collected blocks of laminated mudstone show little indication of systematic change in thickness.

The laminae are commonly ungraded, but some are normally graded and a few are inversely graded (Figs. 7A, B). Backscatter images show abrupt contacts between layers of similar silt grade but with different degrees of compaction and proportion of clay (Figs. 7C–F). Low-angle cross-lamination is rarely present in the yellow laminae (Fig. 6A), and no evidence of desiccation features or bioturbation was noted. Laminar contacts are planar- or wavy-parallel (Fig. 6B), and minor scours up to 0.5 cm deep are filled with different-colored laminae (Fig. 6A, B). Load casts and overturned beds are present where gray laminae overlie interbedded yellow and red-brown layers (Fig. 6A).

Normal microfaults with a vertical extent of 1 cm contort the layers and commonly terminate within gray laminae (Figs. 6A, 7B). Loop bedding is present where laminae up to 0.5 cm thick wedge out along low-angle discontinuities, ranging from simple structures with laminae bending symmetrically on both sides of a boudin neck to complex loops with faulted boudin necks (Fig. 6B; Calvo et al. 1998). Roll-over geometries are preserved with slight draping over some microfaults (Fig. 7B). Microfaults and loop bedding are more prominent in the uppermost 70 cm, yielding an upward change from parallel to wavy lamination.

Complete and fragmentary permineralized plant leaves, branches, and stems (up to 15 cm long and 4 cm wide) are preserved in the laminated mudstone. It is unclear whether the plant remains lie preferentially on the tops or the bases of the laminae, but they are common in red-brown layers, and yellow layers viewed in thin section contain greenish black patches at lamina tops or in the layers, attributed to plant fragments (Fig. 7B). One blattoid insect wing was identified, and a few indeterminate three-toed footprints and discontinuous surface marks in the lowermost part of the unit are attributed to fish or amphibians, probably swimming traces.

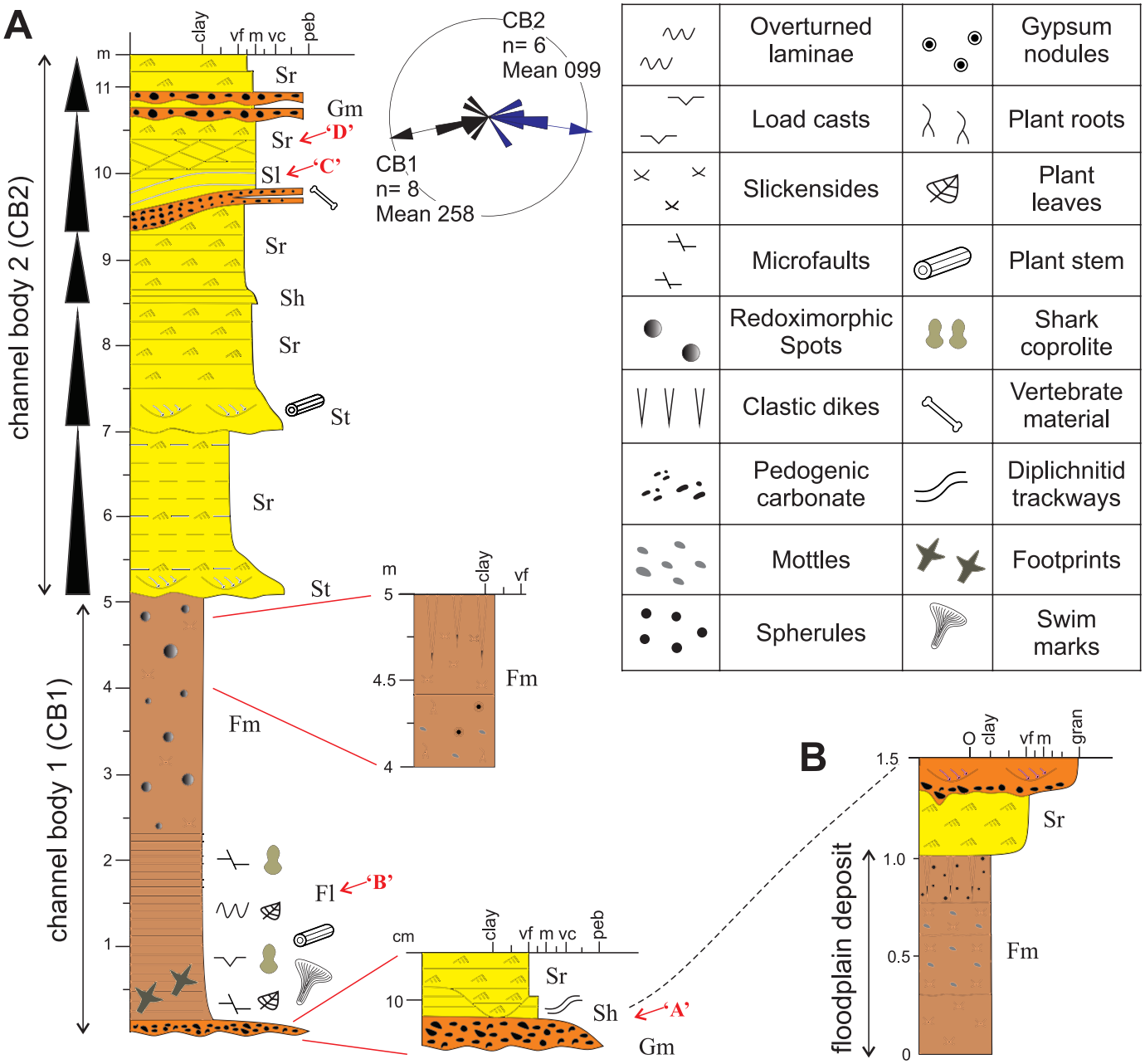

FIG. 3.—Lithological logs at Colwell Creek Pond. **A)** Log illustrating the sedimentological features of Channel Bodies 1 and 2. A detailed section of the basal 20 cm and upper 1 m of Channel Body 1 are also shown. Five fining-upward cycles are noted in Channel Body 2 by black-filled triangles. The rose diagram represents ripple cross-lamination, with mean westward and eastward paleoflow for Channel Bodies 1 and 2, respectively. Sand grain size: vf, very fine; m, medium; vc, very coarse; gravel grain size: gran, granule; peb, pebble. **B)** Log of floodplain deposits below Channel Body 1 with position shown in Figure 2B.

Coprolites up to 5 cm long are uncommon, and are provisionally attributed to xenacanth sharks, which are known from numerous sites in the formation (Murry and Johnson 1987; Johnson 2012).

Based on XRD, the laminae comprise quartz, undifferentiated feldspar, hematite, goethite, titania minerals, illite, kaolinite, Fe-rich chlorite, and mixed-layer clay (Fig. 8A, B). As used here, illite includes muscovite and hydromuscovite. The gray (CC 4a and 4c) and brown (CC 3r, 4d, and 4e) laminae have similar spectra and contain a higher proportion of quartz, feldspar, and illite than the yellow laminae (CC 1a, 1b, 1c, and 3j). Goethite was only identified in yellow laminae, and a fossilized plant preserved on a yellow lamina surface (CC 1b) yielded the strongest peak intensities for goethite. The leaves were rarely preserved as a carbonaceous film surrounded by a bluish gray zone of reduced iron. All samples had less than 0.27% carbon, with an average of 0.17% (Table 2). The carbon content showed no apparent correlation with color, and total organic carbon was virtually identical to the total carbon, indicating that inorganic carbon (for example, carbonate) was minimal or absent.

Interpretation.—Based on the fine grain size and grading, the silt-to-clay laminae are attributed to flows that entered standing water within the water column or along the bed, with deposition under waning flow.

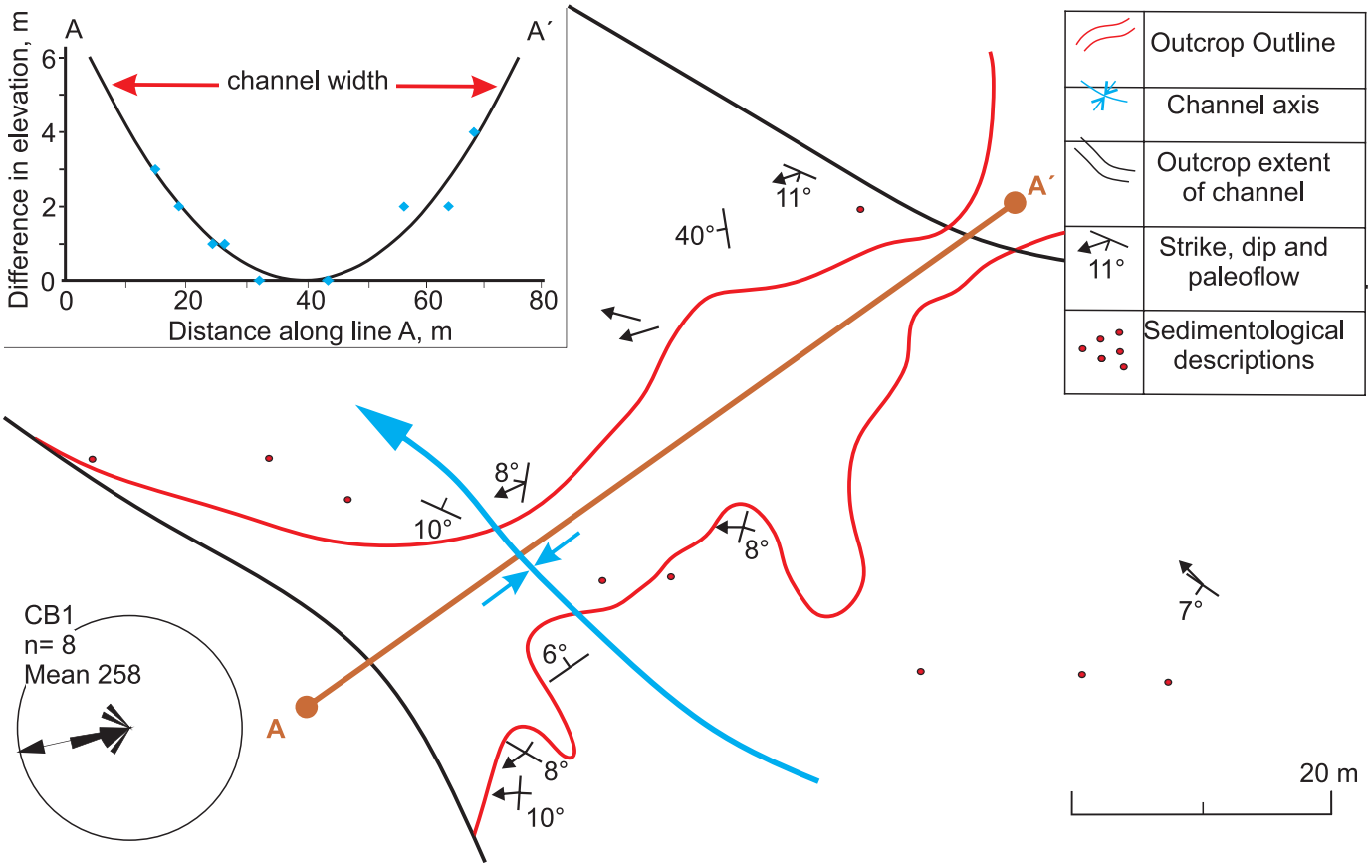

FIG. 4.—**A)** Map of Channel Body 1 at Colwell Creek Pond, showing the outcrop outline and the traceable extent of the channel margin. Circles represent sites with sedimentological descriptions and GPS locations, with strike and dip and paleoflow data from other sites. Line AA′ is perpendicular to the channel axis, with the original inferred SW edge of the channel defined as Point A. The rose diagram for Channel Body 1 is also shown. **B)** Cross section AA′ of Channel Body 1. Using a parabolic model, a thickness of 5 m produces a channel width of 65 m. If 1 m of section in Channel Body 1 was eroded below the overlying channel body, the minimum channel width would have been 72 m.

Generally flat and non-erosional contacts imply weak currents, but currents were periodically strong enough to transport bedload (ripple cross-laminated lenses) and erode scours, and inverse grading suggests velocity reversals. The coarser-grained and thicker laminae low in the unit suggest stronger initial flows.

Loop bedding (see Calvo et al. 1998) has been attributed to desiccation (Bradley 1931), synaeresis, or diagenetic cracking (Donovan and Foster 1972; Cole and Picard 1975), extensional stress (Dean and Fouch 1983), seismicity (Hesselbo and Trewin 1984), shear stress produced by turbidity currents (Trewin 1986), and gas-bubble leakage (Fregenal-Martinez and Melendez 1994). Calvo et al. (1998) inferred an interplay between ductile deformation during lithification and extensional stress (micro-seismic shocks from tectonic activity), acting on competency differences between layers. Based on the minimal degree of deformation of the Clear Fork Formation and a quiescent Permian tectonic setting (Nelson et al. 2013), seismic effects and extensional stress are improbable causes of loop formation. No evidence was found for desiccation or bubble effects, and flows appear to have been gentle. Consequently, loop bedding and microfaults are attributed to near-surface compaction, and their association with load casts and overturned laminae indicate partial consolidation; textural heterogeneity (Fig. 7) may have provided competency contrasts. The up-section increase in deformational features may reflect in part progressive drying and stress as the channel filled.

Massive Mudstone (Fm)

Description.—At the top of Channel Body 1 (Figs. 2A, 3), 2.9 m of red-brown, noncalcareous massive to weakly stratified mudstone rests sharply but non-erosionally on laminated mudstone. It is relatively consolidated but more friable below Channel Body 2. In the topmost meter, the lowermost 40 cm has a coarse, angular blocky structure with discontinuous clay skins coating the surfaces and gypsum nodules in the basal part. A prominent feature is the abundance of vertical drab mottles that branch downward, up to 2 cm wide and 20 cm long. The uppermost 60 cm grades up to a finer blocky structure, with slickenplanes and clay skins that are independent of each other. Sandstone dikes taper down from the base of Channel Body 2. Reduction spherules are prominent throughout.

Below the margin of Channel Body 1 (Fig. 2B), 1 m of mudstone is yellowish red below to more intensely red above, noncalcareous, and divided into sub-units at wavy boundaries. Slickenplanes have well-oriented clay skins along their surfaces, with drab mottles and reduction spherules. The topmost part has an angular blocky structure with clastic dikes below ripple cross-laminated sandstone. Four randomly oriented bulk samples have a similar composition to that of the laminated mudstone, each with quartz, feldspar, titania minerals, and trace amounts of hematite. In the < 2 μm fraction, illite, kaolinite, and Fe-rich chlorite predominate, with traces of mixed-layer clay and goethite. Minor dolomite was identified in one sample.

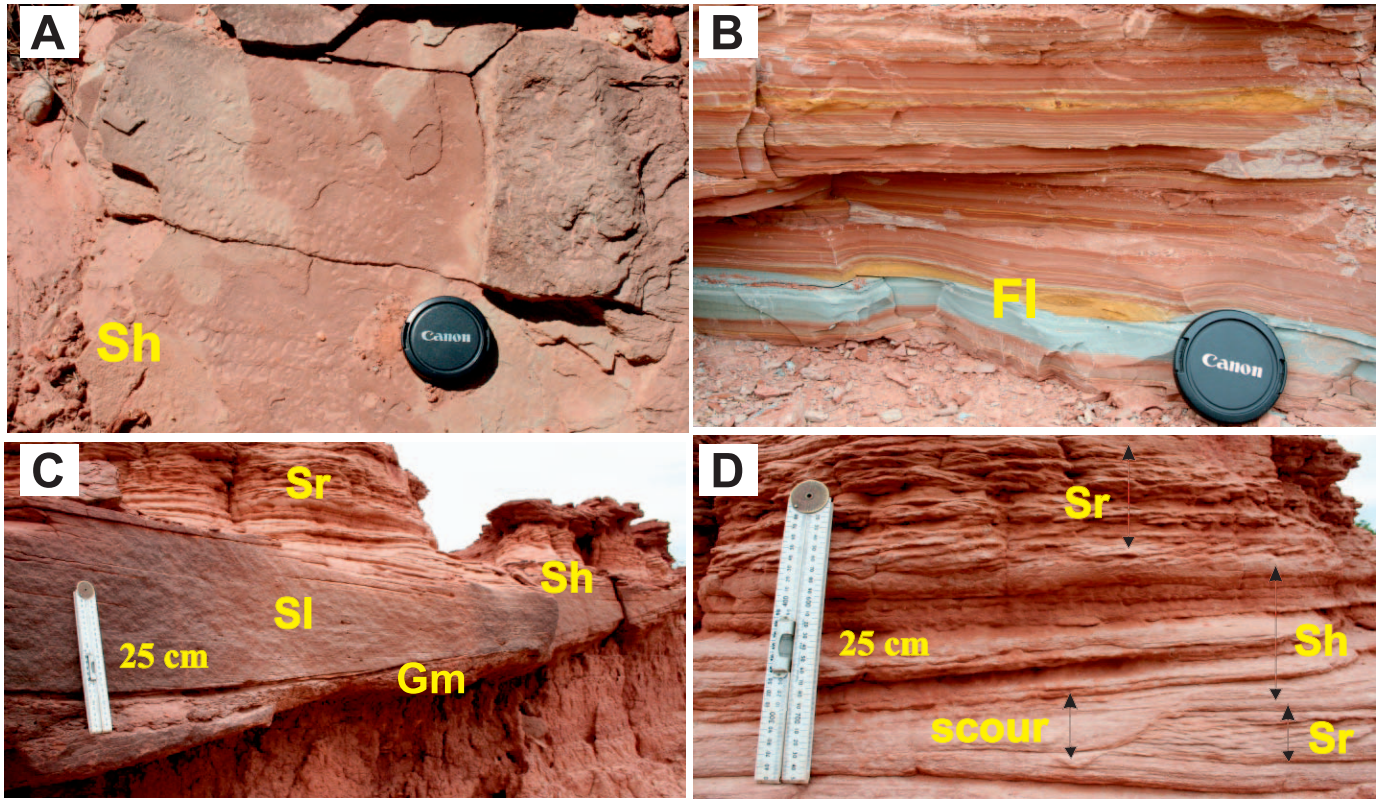

FIG. 5.—Field photos. Diameter of lens cap is 6 cm. **A)** Plane beds with trackways of *Diplichnites gouldi* in basal deposits of Channel Body 1. **B)** Variegated, laminated mudstone (Fl), close to the base of Channel Body 1. **C)** Antidune bedform (Sl) in the fourth cycle of Channel Body 2, resting on a thin lens of pebble conglomerate (Gm) and passing laterally into plane beds (Sh) and upwards into ripple cross-laminated beds (Sr). **D)** Close-up of the upper part of the fourth cycle. Smaller rhythms comprise alternate layers of plane beds (Sh) and ripple cross-lamination (climbing and nonclimbing, Sr), with scour fills. The positions of photos are noted on the logs in Figure 3.

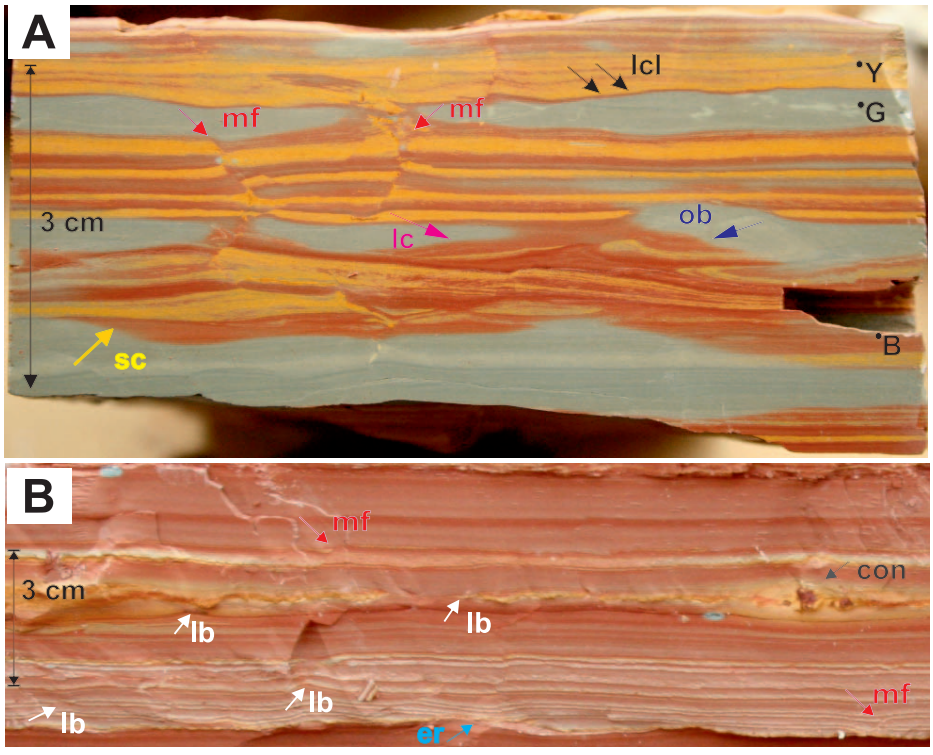

FIG. 6.—Syn- and post-deformational features in the laminated mudstone of Channel Body 1. **A)** Interbedded red-brown "B" and yellow "Y" layers are truncated by normal microfaults (mf), which terminate in the overlying or underlying gray "G" laminae. Load casts (lc) are visible in the gray layers, and the underlying interbedded red-brown and yellow layers are commonly overturned (ob). The bases of the laminae are locally scoured (sc), and low-angle cross-lamination (lcl) is observed in yellow laminae. **B)** Laminated beds with loop bedding (lb) and microfaults (mf). Laminae bases are mainly non-erosional planar- or wavy-parallel; in rare cases, the bedding contacts are irregular and erosional (er). Concretions (con) around permineralized plant leaves are common in the yellow laminae.

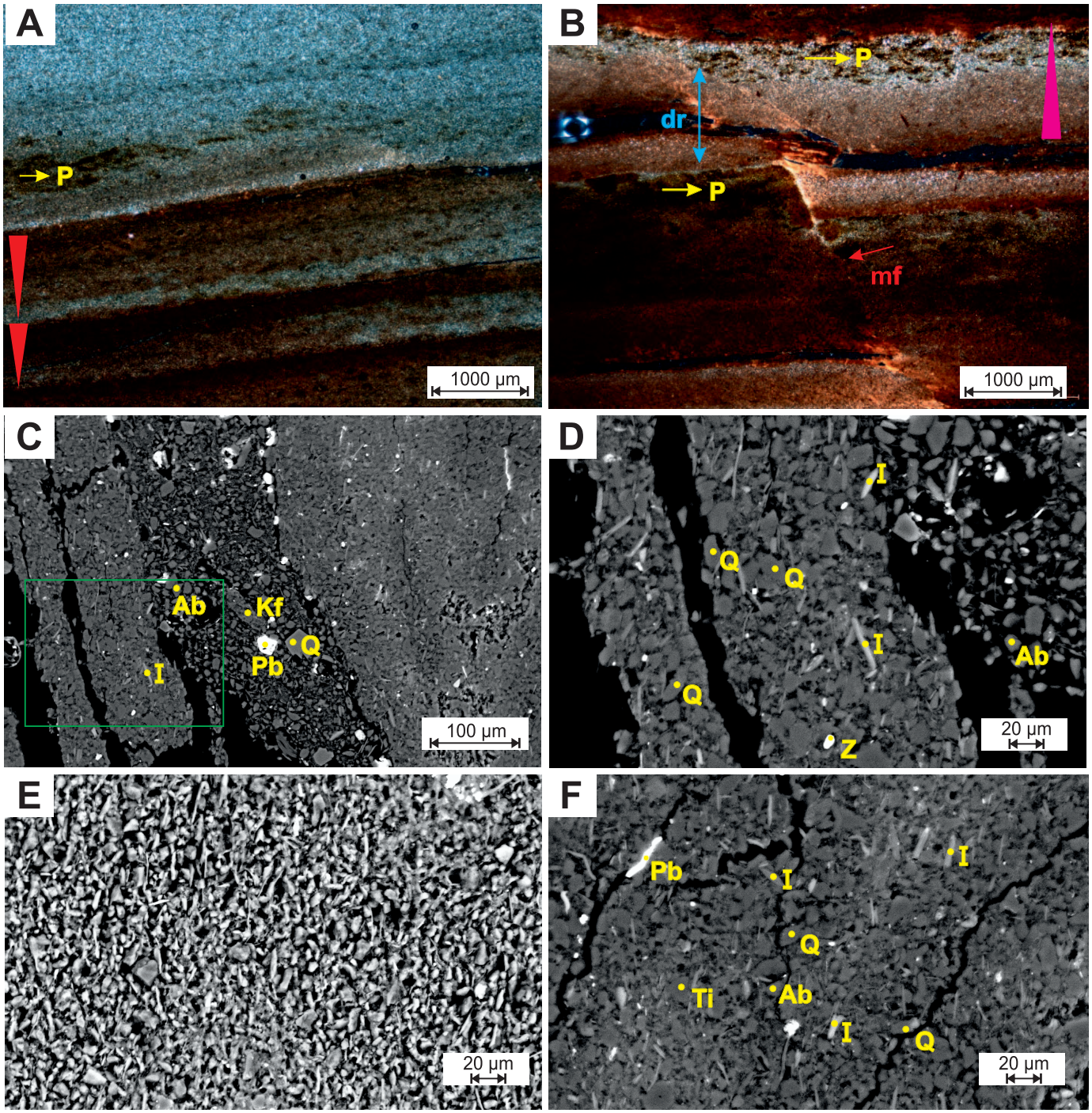

FIG. 7.—Photomicrographs of laminated mudstone (facies Fl) in plane-polarized light (A, B) and as SEM backscatter images of polished thin sections (C–F). **A)** Planar-laminated mudstone with graded bedding (red arrows) and quasi-horizontal to concave-downward bedding surfaces. Dark particles (P) present discontinuously along the laminae are interpreted as plant fragments. **B)** Microfaults (mf) cutting laminae, with draping (dr) of overlying sediments across the fault trace. The overlying laminae are variously ungraded or inversely graded (pink arrow). **C)** Layers with distinct textures and sharp boundaries, with coarse silt-size grains in a loosely compacted lamina at center. In the more compacted layer at right, irregular pits are a product of the thin-section preparation process. White fragments (Pb), commonly along fractures, are contaminants from lead block used in the thin-section preparation. **D)** Close-up of area in the green box in Part C, showing silt-size grains of varied composition. **E**, **F)** Abundant silt-size (medium to fine) grains and clay matrix. Q, quartz; Ab, albite; Kf, K-feldspar; I, illite with bladed habit; Z, zircon; Ti, titania minerals.

Interpretation.—Based on remnant stratification, the facies is inferred to have formed from suspension in standing water in a channel or on a broader floodplain. Following improved drainage and aeration, pedogenic processes obliterated structures as paleosols developed. The vertical drab mottles, especially prominent in Channel Body 1, are interpreted as haloes around former roots that aided the destruction of stratification. The clastic dikes are inferred to have filled desiccation cracks. For both paleosol profiles, slickenplanes, clay skins, gleyed

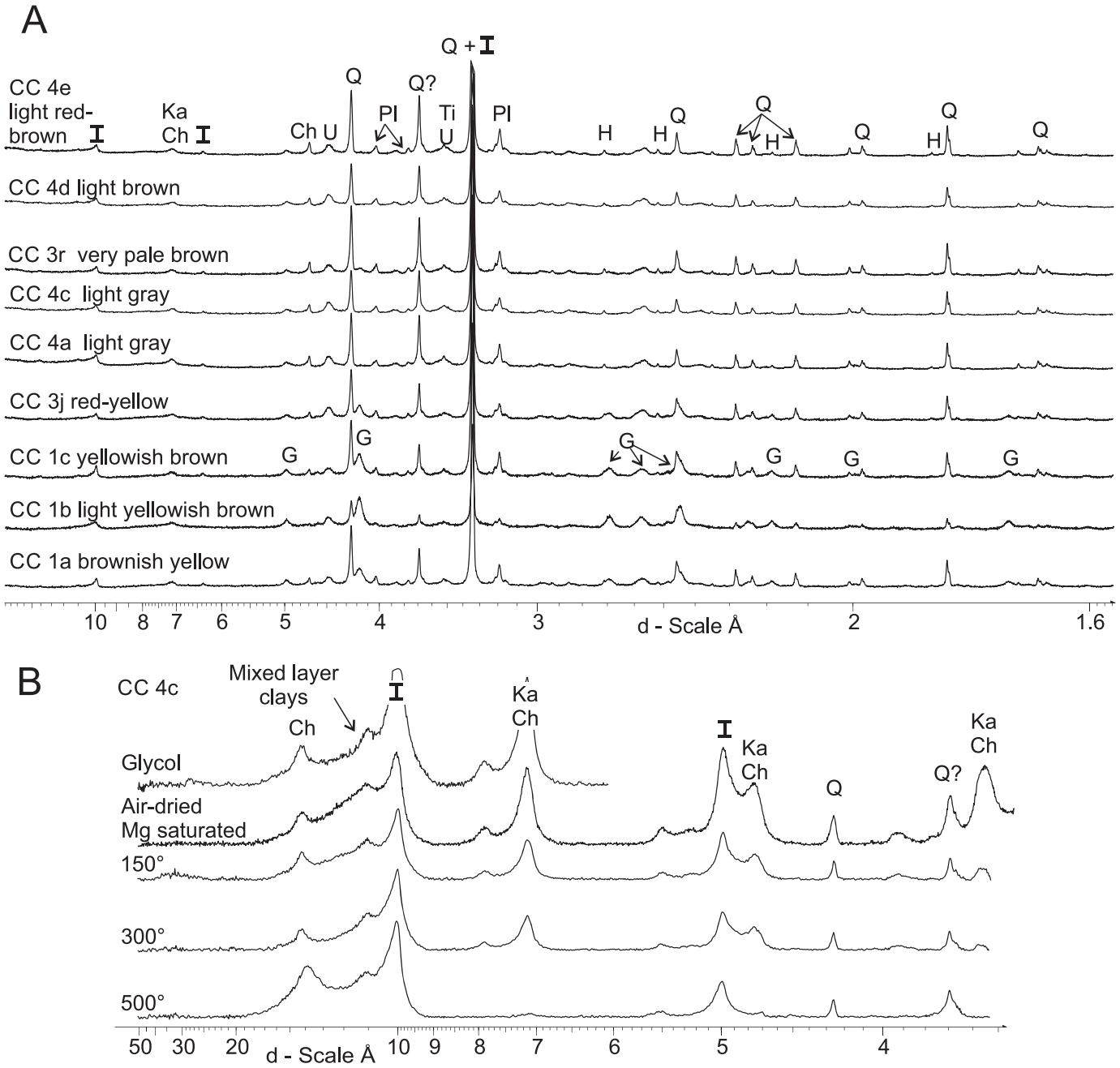

FIG. 8.—X-ray diffraction spectra for < 2 μm nonoriented samples of laminated mudstone. **A)** Nine spectra for individual laminae, arranged by color (see Table 2). Criteria used for mineral identification are shown in Table 3. Samples CC 4a, 4c, 3r, 4d, and 4e are composed of illite, kaolinite, chlorite, undifferentiated clays, quartz, feldspar, hematite, and titania minerals. Samples CC 1a, 1b, 1c, and 3j also contain goethite; sample CC 1b has the strongest peak intensities for goethite. **B)** Diffractograms of the < 2 μm clay fraction in CC 4c, showing the effects of heat treatment and glycolation, with identification of chlorite, kaolinite, illite, and mixed-layer clays. Q, quartz; Pl, plagioclase; I, illite; Ch, chlorite; Ka, kaolinite; U, undifferentiated clays; Ti, titania minerals; H, hematite; G, goethite.

mottles, and desiccation cracks suggest a seasonal climate with wetting and drying that, in sediment with mixed-layer clays, resulted in shrink–swell features.

Facies Fm resembles Pedotype G of the Clear Fork Formation, attributed by DiMichele et al. (2006) to Vertisols formed in floodplain muds. This pedotype consists of red-to-brown claystone with wedge-shaped aggregates, slickensides, and clastic dikes, indicating episodic shrink–swell processes. The clay-mineral (< 2 μm) fraction in Pedotype G is dominated by smectite, trace kaolinite, and weathered micas (DiMichele et al. 2006). The presence of gypsum in the upper part of Channel Body 1 suggests comparison with gypsum-bearing soils of the Mississippi Valley, U.S.A., which formed in a humid but strongly seasonal climate (Aslan and Autin 1998). The origin of the minor dolomite in one sample is not clear, but dolomite-cemented sandstones and paleosols are prominent at other Clear Fork localities (S. Simon, unpublished data) and in Early Permian paleosols elsewhere in the region (Kessler et al. 2001). As discussed more fully under Paleoclimate, below, dolomitic paleosols are widely inferred to represent evaporative groundwater conditions.

TABLE 2.—*Summary of technical information for nine individual laminae in laminated mudstone (facies Fl).*

Sample	Munsell Color	Description	Total Carbon (TC %)	Total Organic Carbon (TOC %)
CC 3j	7.5YR 6/6	Reddish yellow	0.27	0.27
CC 1a	10YR 6/6	Brownish yellow	0.15	0.14
CC 1b	10YR 6/4	Light yellowish brown	0.20	0.20
CC 1c	10YR 5/8	Yellowish brown	0.18	0.18
CC 3r	10YR 7/4	Very pale brown	0.17	0.17
CC 4d	7.5YR 6/3	Light brown	0.09	0.09
CC 4e	5YR 6/4	Light reddish brown	0.13	0.13
CC 4a	Gley1 7-8/N	Light gray	0.23	0.23
CC 4c	Gley1 7-8/N	Light gray	0.11	0.08
		Average	**0.17**	**0.017**

Especially in Channel Body 1, facies Fm differs from Pedotype G in the abundance of drab vertical mottles. In this respect the facies more closely resembles Pedotype D (DiMichele et al. 2006), interpreted as paleo-Vertisols in the underlying Markley and Archer City formations, for which redox effects were attributed to a shallow water table and a relatively humid paleoclimate; this is discussed further below.

Other Facies

Five standard fluvial facies comprise Channel Body 2 and form a minor component at the base of Channel Body 1 (Table 1). *Pebble conglomerate (Gm)* forms units up to 25 cm thick of angular 2–3 cm fragments of gray dolomitic carbonate, and local mudstone chips, with Fe-oxide staining and rare indeterminate bone fragments. The units can be traced laterally for up to 5 m and are largely massive with a few 15 cm trough cross-beds. The facies rests erosionally on red siltstone of facies Fm at the base of Channel Body 1 and on sandstones in Channel Body 2, and is interpreted as a channel lag of intrabasinal material eroded from paleosols adjacent to the channels or upstream. The presence of dolomite in the floodplain paleosols of facies Fm supports a paleosol origin for the dolomitic clasts, although alteration from carbonate precursors during shallow burial cannot be ruled out. Bone material may have been derived from organisms in the channel or reworked from floodplains or paleosols.

Planar-stratified sandstone (Sh) comprises gray planar laminasets with current lineation, up to 10 cm thick. Trackways of *Diplichnites gouldi* (Gevers et al. 1971) up to 3 cm wide and 30 cm long are prominent at the base of Channel Body 1 and are oriented near parallel or oblique to the lineation (Fig. 5A). Units are discontinuous and sharply overlie facies Gm and underlie or grade laterally into facies Sr. *Low-angle cross-stratified sandstone (Sl)* forms a red convex-upward mound 50 cm thick in Channel Body 2, with form-concordant, low-angle stratification and an extent of 3 m within a scour. The bed rests abruptly on facies Gm and wedges out against and passes up into facies Sh (Fig. 5C). Both facies are attributed to upper-regime flow conditions, with the Sl mound formed as an antidune bedform when Froude numbers for transcritical and supercritical flows were exceeded (Langford and Bracken 1987), probably in shallow water (Allen et al. 2013). Rapid discharge decline may have prevented reworking of the antidune into lower-regime bedforms (Alexander and Fielding 1997; Fielding 2006). The diplichnitid trackways in Sh were made by arthropods (Minter et al. 2007) that moved along the current direction, probably as flow waned.

Trough cross-bedded sandstone (St) forms 40 cm units in Channel Body 2, with 20 cm trough sets, mudstone clasts, and one indeterminate plant stem 10 cm long and 1 cm wide. *Ripple cross-laminated sandstone (Sr)* consists of gray or red cross-laminated sets up to 3 cm thick that are locally climbing and show FeMn oxide staining and redoximorphic spots. At the base of Channel Body 1, lenses 10 cm thick rest erosionally on other coarse facies, thickening to 40 cm in scours and overlain abruptly by facies Fl. In Channel Body 2, Sr forms units up to 1.5 m thick that rest abruptly or gradationally on facies St or Sh and locally pass upward from climbing to nonclimbing sets (Fig. 5D). Both facies St and Sr formed in the lower flow regime, as sinuously-crested dunes and ripples, respectively. For Sr, an upward transition from climbing to nonclimbing ripples represents progressively reduced aggradation of suspended sediment as flow strength declined, with thick beds indicating an abundant suspended load.

FACIES ARCHITECTURE AND PALEOFLOW

Channel Body 1 is 5 m thick above an erosional surface overlain by a thin, discontinuous layer of coarse deposits (Gm, Sh, Sr) formed during incision and initial flow. The remaining 4.5 m of the channel fill comprises mudstone (Fl overlain by Fm). A map of the basal contact outlines a linear channel with an axial position estimated from dip variations in the basal beds (Fig. 3). Elevation measurements indicate a concave-upward basal surface and a channel width of 65 m at the top of the preserved fill, based on a parabolic model. This suggests a width: thickness ratio for the channel body of 13:1, a "broad ribbon" geometry (Fig. 3; Gibling 2006). Erosion below Channel Body 2 probably removed the topmost fill of facies Fm, which may have overlapped the margin to merge with floodplain deposits. A westward paleoflow for the basal beds appears oblique to the channel margin, suggesting deflection off the eastern bank.

Channel Body 2 is 6.5 m thick, with its topmost strata eroded, and comprises five erosionally based cycles, each 1–2 m thick, that fine upward from granule and/or pebble conglomerate to very fine-grained sandstone. In the sandstone, trough cross-beds (St) grade upward into plane beds (Sh) and climbing and nonclimbing ripple cross-lamination (Sr), indicating waning flow strength. In the fourth cycle, a basal erosional surface draped by lenses of pedogenic carbonate and mudstone clasts (Gm) with bone fragments is overlain by an antidune (Sl), overlain in turn by plane beds (Sh) and climbing and nonclimbing ripples (Sr) (Figs. 3A, 5D). The basal surface is planar across the exposure, which is oriented normal to the eastward paleoflow, and the channel body is probably sheet-like.

PLANT FOSSILS

Description.—Three common taxa (walchian conifers, *Taeniopteris*, and *Auritifolia*) account for $>$ 85% of the macrofloral foliage (Fig. 9A–G; Schachat et al. 2014). They were produced by seed plants, and their photosynthetic organs (branches or leaves) show varying degrees of robust construction. The most common floral elements are penultimate branch systems of so-called walchian conifers, an extinct paraphyletic group of small trees with a plagiotropic branching pattern. These branch systems were abscised as single units with ultimate branchlets, and their leaves still attached (Fig. 9A; Looy 2013). The leaves on the ultimate branchlets are

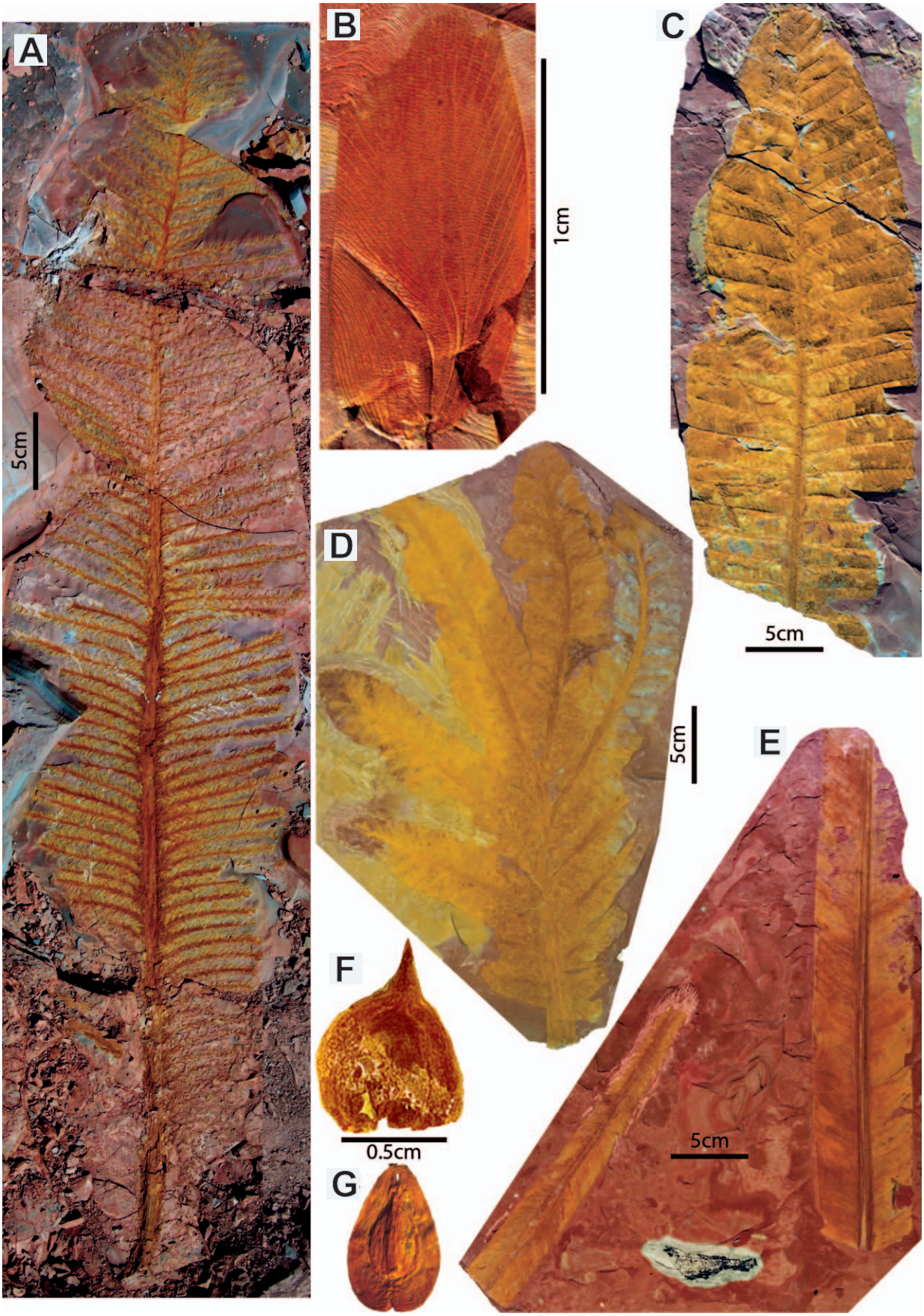
A
5cm
B
1cm
C
5cm
D
5cm
E
5cm
F
0.5cm
G

bifacially flattened, ovate to awl-shaped, and distally incurved. Based on the distribution of variability of gross morphological features among these leaves, Looy and Duijnstee (2013) recognized four walchian "morphotypes" in the deposit, possibly unique species.

Taeniopteris sensu lato is nearly as common as the conifers (Fig. 9E). This is a polyphyletic taxon that, in this deposit, consists mainly of foliage likely attributable to cycadophytic seed plants. The form most typical of *Taeniopteris sensu stricto* (Remy and Remy 1975) has elongated leaves with lateral veins that run nearly at right angles from the midvein to the leaf margin. A second form has large leaves (long and relatively wide) with venation that is much more angular in its insertion than is typical of the genus. It resembles *Lesleya*, although the veins are less flexuose than is typical of that genus (see discussion of the differences between *Taeniopteris* and *Lesleya* in Bashforth et al. in press). The third form of *Taeniopteris* is rare in the deposit and undescribed in the literature. The leaves are small with straight, right-angle, lateral veins that are widely spaced and forked near the midrib. They are of uncertain affinity and may be attributable to ferns or could represent specialized leaves associated with (unrecognized) reproductive organs (or possibly caducous pinnules). All forms of *Taeniopteris sensu lato* at the study site appear to have been leathery in construction, indicative of long-lived leaves.

Third in abundance, but also common, is the comioid *Auritifolia waggoneri* (Fig. 9D; Chaney et al. 2009), a seed plant of possibly peltaspermous affinity. *Auritifolia waggoneri* has a pinnate leaf with distinctive fasciculate venation, similar to that of the genus *Comia* (Mamay et al. 2009), but within which are vein reticulations. Leaves were of robust construction with thick, woody petioles, suggesting that they stayed on the parent for several growing seasons.

Less common seed plants include *Nanshanopteris*, *Evolsonia*, *Supaia*, *Rhachiphyllum*, *Cordaites*, and cf. *Mixoneura*. The suspect peltaspermous affinity of many of these plants, based on their leaf architectures and venation patterns, is noteworthy. The peltasperms appear to have undergone a broad evolutionary radiation during the Early Permian in seasonally dry, tropical settings (DiMichele et al. 2005).

Nanshanopteris is a likely peltaspermous seed plant (Wan and Wang 2015), similar to *Brongniartites* of DiMichele et al. (2005), although Naugolnykh (1999) considered *Brongniartites* to be an illegitimate name. It is similar in form and may be closely related to *Glenopteris*, as described by Krings et al. (2005). *Nanshanopteris* has robust, unforked, once pinnate leaves, similar in shape to *Auritifolia waggoneri*, and the foliage likely had a long leaf lifespan. The habitat of the gigantopterid *Evolsonia texana* (Fig. 9C; Mamay 1989), a possibly peltaspermous seed plant, is unknown; some Cathaysian gigantopterids may have had liana habit (Li and Taylor 1998, 1999). Gigantopterids are common in Chinese and North American Permian strata. Whereas most older gigantopterids have distinctly forked leaves, *Evolsonia* leaves are unforked, broad, thick, and likely leathery with reticulate venation. *Supaia* sp., another likely peltasperm, is represented in the flora by a few specimens, one of which is distinctly forked at the base. White (1929) described many species of *Supaia* some of which, similar to the form described here, may belong to a single, morphologically variable species. Because of the small number of specimens in hand, we leave this material undetermined at the species level. The final probable peltasperm is *Rhachiphyllum* (Kerp 1988). Leaves are known to be forked, although that characteristic was not observed in the fragmentary Colwell Creek specimens. On each fork, leaves are twice pinnate; pinnules are flat, with steeply ascending veins and a weakly developed midrib that crosses the pinnule at an angle, macroscopically, from base to tip. Some veins originate from the rachis (rachial veins) rather than the pinnule midrib. In addition, an important character for identification is the presence of rachial pinnules, borne on the higher-order rachis between the ultimate pinnae.

Cordaites is the foliage of a group of woody seed plants closely related to the conifers (Florin 1954; Rothwell 1982). Leaves are elongate, often strap-like, with parallel veins. As a group, the cordaitaleans had an enormous ecological spectrum, from swamps in shoreline areas (Raymond et al. 2010) to upland regions under conditions of seasonal drought (Falcon-Lang and Bashforth 2005; Bashforth et al. 2014). Their leaves are easily confused in compression preservation with taphonomically flattened rachial axes of marattialean fern and medullosan seed plants, particularly if fragmentary, and are often overlooked.

Seed plants with medullosan affinities are poorly represented in the assemblage. Fragments of pinnules with fine, arcing venation and thin but well developed midveins are most similar to the medullosan seed plant *Mixoneura* (*Odontopteris*). For a recent discussion of this genus, its morphology and taxonomy, see Laveine and Dufour (2013).

Only a single species of an unquestionably pteridophytic plant, *Sphenophyllum* cf. *S. thonii*, was found. This plant is recognized by its distinctively wedge-shaped, multi-veined leaves. A terminal "fringe" of vein endings suggests the *S. thonii* affinity. Stems are jointed with clearly marked, swollen nodes. By analogy with other species of this genus (Batenburg 1982), *S. thonii* most likely was a scrambling, groundcover plant. As such, it is the only plant with that habit that has been identified in the flora. The paucity of groundcover elements, both taxonomically and in terms of abundance, in the fossil assemblage may be a taphonomic happenstance; this pattern is typical of many fossil assemblages and has been attributed to protection of small plants from the effects of wind as a natural sampling agent (Scheihing 1980). Alternatively, it is possible that there was little groundcover surrounding the site.

Interpretation of Life Setting.—The seed plants at the study site almost uniformly produced leaves that lived for more than a single season or, in the case of conifers, lateral branches with similar extended life spans. The leaves of *Evolsonia*, *Auritifolia*, and *Taeniopteris* are thick, large, and woody at the base or throughout; leaf thicknesses, measured from permineralized specimens, range from 200 to 250 μm. The branches of Colwell Creek walchian conifers appear to have formed over several seasons of growth, indicated by growth interruption points. In addition, a life span of several years is strongly suggested by woodiness and basal thickening of the branch bases (Looy 2013). Increasingly, physiological studies of conifers with similar types of leaves show that they are mesic to tropical in their tolerances and do not prosper with water deficits (Pitterman et al. 2012). The above-mentioned groups are the four most abundant taxa in the flora (Schachat et al. 2014). These features point to a flora that, by modern standards, would be characterized as physiologically slow, within the leaf economics spectrum (Wright et al. 2004). The large size of these photosynthetic organs also suggests a large potential for transpiration and water loss, indicating that they grew in an environment with nearly year-round groundwater accessible to plants large enough to access this water source.

←

FIG. 9.—Plant and other fossils from laminated mudstone at the Colwell Creek Pond locality. **A)** Walchian conifer branch system (Looy and Duijnstee 2013). Morphotype IV photographed in the field before extraction (USNM 536456). This image is a composite of a series of images. **B)** Blattoid wing (USNM 543850a). **C)** *Evolsonia texana* (USNM 528205b). **D)** *Auritifolia waggoneri* (USNM 508135). **E)** cf. *Taeniopteris*. Foliage similar to *Taeniopteris* in overall shape and in its open, dichotomous venation, however, venation angle falls outside that typical of the genus and may be indicative of a new taxon. (right: USNM 526033; left: USNM 530900). **F)** Type 1 seed (USNM 530907). **G)** Type 2 seed (USNM 539373).

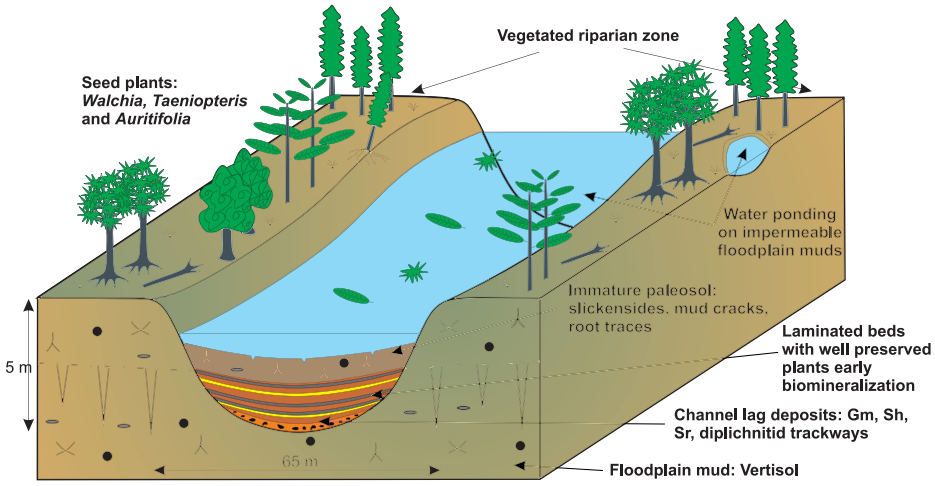

FIG. 10.—Schematic diagram showing the paleoenvironment of Channel Body 1.

None of the plants represented in the flora appear to have been growing in swampy habitats. There are no tree ferns, lycopsids, or calamitalean sphenopsids, typical of equatorial regions of Pangea with high water tables but also of seasonally dry regions where sufficient moisture and occasional standing water supported their requirements (DiMichele et al. 2006). Their absence is, in fact, surprising. Wet-substrate plants, particularly tree ferns and calamitaleans, are known from numerous other deposits in the Leonardian redbeds of Texas, including sites younger than Colwell Creek Pond and much less intensely sampled. They also are known throughout western Pangea, locally in seasonally dry areas within or bordering channels (e.g., DiMichele et al. 2014), and appear to have reached even small wetland sites by virtue of their highly wind-dispersible propagules. It might be concluded, therefore, that their absence at Colwell Creek Pond is just a natural sampling happenstance. However, plant remains in abandoned channels almost invariably are drawn from the immediately surrounding area (Scheihing and Pfefferkorn 1984; Burnham 1989; Gastaldo 1989), and a largely seed-plant flora could indicate a channel with little or no area along the margins for plants requiring a nearly permanent source of water. Given the excellent preservation and evidence of minimal transport of the organic remains, these wetland plants should be represented if they were present.

We conclude that the flora is representative of the immediately surrounding vegetation, and, even in its suggestion of distinct seasonality, may indicate more mesic conditions than those of the interfluves—areas not represented or poorly represented in the assemblage. These more distant areas were likely populated by the most moisture-stress-resistant floral components, the conifers.

DISCUSSION

Incision and Sedimentation History

For Channel Body 1, it is surprising that the deep basal incision is draped only by thin, discontinuous coarse deposits below laminated fines (Fig. 10). Considerable erosive power would have been necessary to cut such a channel, implying the capability for coarse-sediment transport. Patchy basal deposits are characteristic of many Clear Fork channel bodies, and the scarcity of coarse detritus may represent a long transport distance from source areas to the east or denuded proximal (local to subregional) sources.

During incisional avulsion, flow is diverted from the parent channel onto the floodplain (Mohrig et al. 2000), commonly triggered by rapid alluviation, channel blockage, or high-magnitude floods (Miller 1991; Knighton and Nanson 1993; Slingerland and Smith 2004). If the new channel rejoins a sediment-deficient parent channel downstream, increased erosive power may increase the cross sectional area, thinning or removing entirely the pre-existing channel fill (Smith et al. 2014). In contrast, avulsion by annexation redirects the flow into other active, partially active, and abandoned channels, where part of the original channel fill is likely to be preserved (Morozova and Smith 2000; Slingerland and Smith 2004). With no indication of a pre-existing fill, incisional avulsion is the preferred model for the creation of the Colwell Creek Pond channel. Channel creation may have linked overland flow paths or erosional hollows around trees (cf. Gibling et al. 1998), rather than resulting from a single catastrophic event.

Basal gravel (Gm) overlain by plane-laminated (Sh) and ripple cross-laminated (Sr) sandstone represents waning flow after incision. As indicated by diplichnitid trackways, arthropods were active on the channel floor at this time. Although *Diplichnites* is known from marine and freshwater environments, it is common in freshwater settings (e.g., Buatois et al. 1998; Netto et al. 2009), and *Diplichnites gouldi* has been attributed to continental organisms elsewhere in the Clear Fork Formation (Minter et al. 2007).

The laminated mudstone (Fl) represents the initiation of a standing-water body, essentially a small lake, within the incision. The abrupt incoming and sustained deposition of these beds suggests complete disconnection from the parent channel (Toonen et al. 2012), and the lack of evidence for subaerial exposure, such as desiccation cracks, rainprints, or wind-blown sand, suggests permanent standing water. Sedimentary features indicate deposition from density underflows and suspension (Toonen et al. 2012), probably generated by sediment-charged floodwater from neighboring rivers, rainwater flow along tie channels or floodplain depressions, or bank slumps (Mertes 1997; Rowland et al. 2005; Marren and Woods 2011). Groundwater discharge below a spring line can contribute water to channel systems on distal alluvial plains (Weissmann et al. 2013; Weissmann et al. 2015; Hartley et al. 2013), and this process may have assisted in maintaining standing water for prolonged periods. Retention of water would have been aided by the fine-grained, impermeable nature of underlying floodplain deposits (Marren and Woods 2011), as well as flood-derived clay that can seal channel incisions and reduce seepage into the groundwater (Knighton and Nanson 1994a, 1994b; Cendón et al. 2010). In the arid plains of Cooper Creek, where annual evaporation greatly exceeds precipitation, standing bodies of water (waterholes) above the water table can be retained in the channel over several years before flow recommences (Cendón et al. 2010) and are considered more-or-less permanent (Knighton and Nanson 1994b).

Based on the average lamina thickness, the 203-cm-thick unit contains 2900 laminae. An individual lamina may represent a multiannual or annual flow event (Shanahan et al. 2008; Lojka et al. 2009), or several flows may have taken place during a single year. If flows were annual, the laminated unit would have taken ~ 2900 years to accumulate. Some oxbow lakes may be long-lived: in Sky Lake, in the Mississippi area, 120 cm of sediment was deposited in ~ 3600 years prior to anthropogenic effects (Wren et al. 2008), and an oxbow lake in the Czech Republic lasted for nearly 800 years before the lake filled and became a eutrophic fen (Pokorný et al. 2000). However, we suggest that multiple flooding events occurred in most years, as in many modern seasonal areas, and that the sediments accumulated in much less than 2900 years. Oxbow lakes connected to a main river via tie channels may fill in decades to centuries (Rowland et al. 2005), although the sediment is generally coarser than the laminated beds at Colwell Creek Pond. The upward change to massive mudstone with root traces (Fm) indicates progressive shallowing, probably due to sedimentation within a fixed incision, and vegetation may have enhanced pedogenesis considerably.

In contrast to Channel Body 1, Channel Body 2 represents a major fluvial system with considerable coarse sediment (> 6.5 m) and a sheet-like form. The stacked cycles represent repeated short-lived flow events with high-flow-strength bedforms (plane beds and an antidune) followed by deposition of abundant suspended sediment (climbing ripples). The eastward paleoflow, in contrast to the westward paleoflow of Channel Body 1, remains to be explained in a basin with known topographic uplifts to the north and east (Fig. 1A). Sheet-like channel bodies with a change in paleoflow direction were also observed at two other outcrops in the middle Clear Fork Formation.

Modern and Ancient Analogues

Channel Body 1 is interpreted as an abandoned channel that was part of a meandering system, the predominant fluvial style in the formation (Edwards et al. 1983; Nelson et al. 2013). Partial analogues are found in Quaternary abandoned channels (oxbow lakes) along the Mississippi and Rhine rivers (Guccione 1993; Guccione et al. 1999; Toonen et al. 2012), although these systems have abundant coarse sediment and much larger channels than those of the Clear Fork alluvial plain. These modern oxbows locally contain up to 3 m of laminated dark silty clay to clay with disseminated organic matter and thin sandy silt beds. As the water shallowed, vegetation was established and up to 2 m of dark homogeneous silty clay to clay was laid down, with lamination destroyed by shrink–swell processes and roots. The grain size and lamina thickness of the fills reflect in part the distance downstream from the cutoff, the water depth, and plugging of the upstream part of the oxbow, restricting access to coarser sediment. To date, we have not identified a modern abandoned-channel fill that replicates closely the varicolored laminated mudstone of Channel Body 1.

In the Upper Triassic Chinle Formation, fossiliferous abandoned-channel deposits are composed of < 2 m of dark, laminated carbonaceous mudstone and sandstone (Demko 1995). These fining-upward deposits filled oxbow lakes and moribund channels and are thinly laminated (1–10 mm thick), locally bioturbated, and rooted at the top. In the late Permian Normandien Formation of the Karoo Basin in South Africa, an oxbow-lake fill comprises 3–4 m of olive gray shale with glossopterid leaves and other vascular plant organs (Prevec et al. 2009). Although the shale was not described in detail, the authors suggested that the water body was semiperennial based on the paucity of desiccation features, the thickness of the channel body (25 m), and the presence of discrete sediment packages. In the Early Permian Wichita Group, which underlies the Clear Fork Formation in Texas, gray or yellow lenses in redbeds represent shallow abandoned channels or ponds and contain vertebrate bones and plants (Sander 1987; Hotton et al. 2002; Chaney et al. 2005; Labandeira and Allen 2007). Little information was provided about stratification, but the drab color suggests reducing bottom conditions.

In terms of its stratification, the Colwell Creek Pond mudstone resembles the deposits of some larger modern and ancient stratified lakes. These deposits are variably composed of detrital, carbonate, and organic laminae with vertebrate, invertebrate, and plant material, and the lamination is commonly attributed to annual events or flows that laid down graded beds (Wilson 1977; Ludlam 1981; Gibling et al. 1985; Demicco and Gierlowski-Kordesch 1986; Clausing and Boy 2000; Menounos et al. 2005; Shanahan et al. 2008; Lojka et al. 2009). Although some process inferences may be applicable, such large lakes are not applicable to the study site, which was little more than 5 m deep and a few tens of meters wide. A closer analogue is provided by laminated mudstones in the Miocene Siwalik Group of Pakistan (Zaleha 1997a, 1997b), attributed to short-lived to perennial floodplain lakes less than 10 m deep; however, these deposits contain micritic calcite and sparse trace fossils.

A possible analogue for Channel Body 2 is the ephemeral sheetflow-dominated River Gash in Kassala, Sudan (Abdullatif 1989). This broad, shallow sandbed river has laid down a sheet of coarse sediment and experiences high discharge variations, evaporation, and infiltration in an arid setting. Deposits include cross-beds, plane beds, and scour-and-fill units, with successions laid down during events of high flow strength and waning flow.

Preservation of Lamination

The preservation of laminated mudstone in subaqueous settings is generally related to the impoverishment of benthic fauna, limiting disruption of the laminae (Cohen 1984). Paleozoic freshwater environments were dominated by epifaunal traces (Buatois and Mángano 1993), and infaunal activity is not recorded until the Permo-Triassic, since endobenthos required new ways of obtaining oxygen and completing their reproductive cycles (Miller 1984; Miller and Labandeira 2002). Sites elsewhere in the Clear Fork Formation yield diverse trace fossils characteristic of Early Permian redbeds (Lucas et al. 2011), but the presence of surface traces and the lack of open burrows suggest largely epifaunal communities (Minter et al. 2007).

Reduced benthic populations have also been related to low bottom- or pore-water oxygenation, low productivity, a high sedimentation rate, and elevated salinity (Verschuren 1999; de Gibert and Ekdale 2002). Anoxic conditions at the bottom of a permanently stratified lake is the most common explanation for the absence of bioturbation (Kelts and Hsu 1978; Anderson and Dean 1988). However, Cohen (1984) showed that, in Lake Turkana in Kenya, oxygen-saturated water was present down to the water–sediment interface due to mixing by wind action and the low depth:fetch ratio. At 4 cm below the interface, a sharp decline in oxygen was accompanied by a change from red-brown to olive-green sediment, the latter inferred to be laminated. The scarcity of benthic organisms was attributed to a subsurface oxygen deficit and to the low concentration of organic matter in the sediments, implying a limited food source. Laminae may also be preserved where rapid sediment accumulation outpaces the capacity of the macrobenthos to homogenize the sediment (Verschuren 1999), as inferred for abandoned-channel fills of the Mississippi River by Guccione (1993). Several studies have suggested a correlation between hypersalinity and reduced diversity (Sugden 1963) and an increase in dwarfism (Kinne 1970; Price 1982).

For Miocene laminated lacustrine beds in Pakistan, Zaleha (1997a) suggested that the lake was oxygenated throughout based on wave-ripple cross-lamination and the scarcity of plant detritus. The rarity of organisms and preservation of lamination was attributed to the low availability of organic detritus as a food source, the high sedimentation rate, and chemical factors such as alkalinity, pH, total dissolved solids, and trace elements.

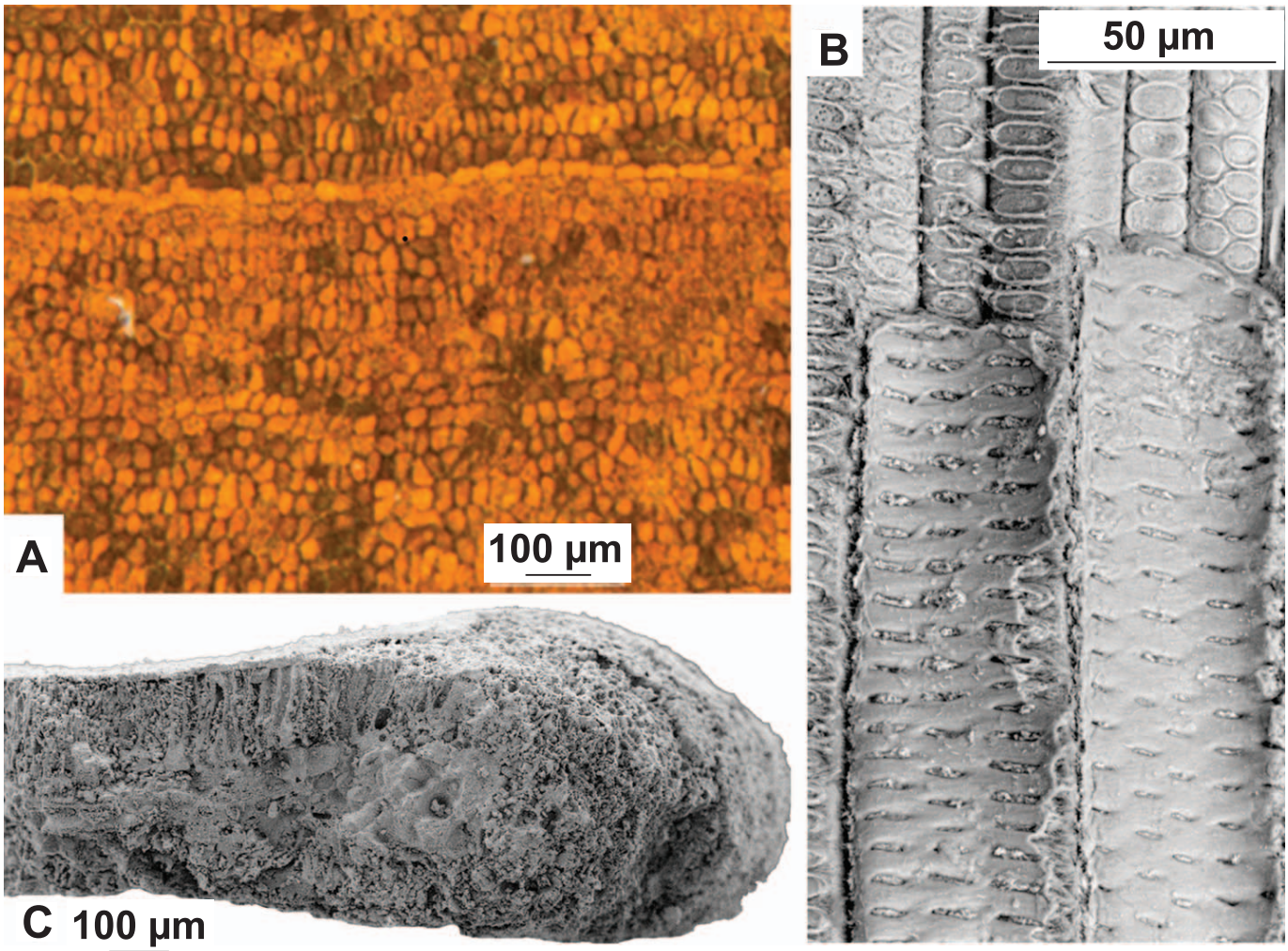

FIG. 11.—Goethite petrification of cellular structure of plant remains recovered at the Colwell Creek Pond locality. **A)** *Taeniopteris* (USNM 539325) true-color image of the adaxial leaf surface. The cuticle was not preserved; the adaxial ends of the palisade cells are visible and grouped into costal and inter-costal bands. **B)** *Taeniopteris* (USNM 539324) SEM micrograph. View of tracheid cells in the main vein of the lamina. Elongate hollow tracheid cells are broken longitudinally, exposing the internal openings to oval bordered pits. **C)** *Auritifolia waggoneri* (USNM 528671) SEM micrograph. View of broken edge of leaf cross section showing the palisade cells, parenchyma, and the lower adaxial epidermis. At the right, the rounded outer edge of the leaf is slightly inflated compared to the internal part of the lamina.

None of these explanations can be entirely supported or ruled out for the Colwell Creek Pond site. We hypothesize that the delayed colonization of freshwater ecospace was an important factor (Miller and Labandeira 2002). Anoxic to dysoxic bottom or subsurface conditions may have prevailed periodically, but the presence of graded beds and other flow features, coprolites and swim marks, and cements of hematite and goethite suggest that bottom water and shallow sediment was mainly oxygenated. The low organic content of the mudstone may imply low productivity in the standing water and limited nutrient availability for benthos, although organic matter is rapidly oxidized on seasonally dry alluvial plains (Sharma et al. 2004). Evidence for active flow suggests that rapid sedimentation assisted in preserving lamination from bioturbation. Petrographic analysis failed to indicate phases associated with elevated salinity or unusual chemical conditions, such as carbonates, evaporites, or unusual clay minerals (e.g., sepiolite, palygorskite). However, calcium carbonate precipitates from sea water only when salinity is $\sim$ 1.8 times normal values (McCaffrey et al. 1987), and elevated salinity need not be accompanied by a mineralogical signature. Although a seawater model is not applicable to the study site, elevated salinity may have excluded benthic organisms but left little other trace. In conclusion, the presence of undisturbed lamination may be attributed to delayed colonization of the abandoned channel by benthos, supplemented by issues of water chemistry, sedimentation, and productivity.

Paleoclimate

Evidence relevant to a paleoclimatic interpretation was obtained at three stratigraphic levels. For floodplain deposits below Channel Body 1, the paleosols are interpreted as paleo-Vertisols formed in seasonal settings, in accord with the presence of mixed-layer clays and desiccation features. A significant observation is the presence of dolomite in the paleosols and reworked pedogenic dolomite nodules in facies Gm at the base of Channel Body 1. Detrital dolomite may have been reworked from the Wichita and Arbuckle Mountains (Ham 1973; Gilbert 1982) or derived as windblown accessions from coeval marine deposits or playa lakes (Petersen et al. 1966; Kessler et al. 2001; DiMichele et al. 2006; Minter et al. 2007). However, an upward transition from early-formed calcite and ankerite cement in the lower member to dolomite and gypsum

TABLE 3.—*Criteria used for identification of minerals during X-ray diffraction analysis (Moore and Reynolds 1997).*

Mineral	Identification
Low quartz	Characteristic 100 and 101 reflections at 4.26 Å and 3.34 Å. An anomalous peak at 3.7 Å is provisionally attributed to quartz based on the examination of 75 spectra from the Clear Fork Formation in which the intensity of this peak is similar to that of the quartz 100 reflection and it occurs only when quartz is present in the sample.
Feldspar	Characteristic peaks at 3.20 Å, 3.7–3.83 Å, 4.0–4.1 Å, and 6.3–6.6 Å.
Dolomite	Characteristic 104 reflection at 2.89 Å.
Hematite	Weak and broad 104 and 110 reflections at 2.69 Å and 2.52 Å, reflecting the low degree of crystallinity.
Goethite	Strong 110 reflection at 4.18 Å with broad 130 and 021 peaks at 2.69 Å and 2.58 Å.
Ti-oxide	Weak 101 reflection occurs at 3.51–3.52 Å.
Illite	Characteristic 001, 002, and 003 reflections at 10.1 Å, 4.99 Å, and 3.38 Å; the latter peak overlaps with the low quartz 101 reflection. Upon glycolation, the 10.1 Å peak becomes sharper with increased intensity, suggesting the presence of expandable clays. The ratio of the d-spacing (001) and (002) reflectors was greater than 2.00, which indicates that the illite shows some degree of interstratification with other clay minerals.
Chlorite	Characteristic 001, 002, 003, and 004 reflections at 14.4 Å, 7.15 Å, 4.77 Å, and 3.55 Å, respectively. The chlorite peak positions slightly sharpened by glycolation (presence of expandable clays), but the 001 reflection increased dramatically in intensity, while the other peaks were weakened during heating to temperatures > 300°C. Since the odd-order peaks (001, 003, and 005) have lower intensities than the even-order peaks (002 and 004) and the intensity of chlorite 001 peak is less than the 003 peak, the chlorite minerals are enriched in iron in the hydroxide layer.
Kaolinite	Characteristic 001 and 002 peaks at 7.18 and 3.58 Å overlap with the chlorite 002 and 004 peaks.
Mixed layer clays	Mixed layer clays not identified within this study but are present between 11 and 13 Å, and a broad, weak peak appears between 30 and 40 Å when the sample is heated to 150°C.
Standard Zincite	Characteristic 100, 002, 102, and 110 reflections at 2.81 Å, 2.60 Å, 2.47 Å, and 1.62 Å, respectively.

cement in the middle and upper members (S. Simon, unpublished data) implies increasingly evaporative groundwater conditions which would have elevated Mg/Ca and promoted dolomite formation (cf. Arakel and McConchie 1982; Spötl and Wright 1992; Colson and Cojan 1996; Schmid et al. 2006). Notwithstanding a possible contribution from reworked dolomite, the stratigraphic evolution of the groundwater suggests relatively arid conditions.

For Channel Body 1, the laminated beds represent a standing-water body with no indication of desiccation over a period of centuries to a few millennia. XRD analysis indicates a terrigenous composition and the water may have been fresh, although a modest salinity increase could have gone unrecorded. Invertebrate traces are restricted to arthropod trackways, and although this suggests an inimical environment, these were early days in the colonization of benthic freshwater settings. Non-moisture-limited conditions are indicated by seed plants with large, robust thick leaves, suggesting that the parent plants grew in riparian settings where they experienced periodic moisture stress but had access to groundwater nearly year round. A puzzling point is that the assemblage lacks plant groups characteristic elsewhere of seasonally dry settings where water sources were locally available. Paleo-Vertisols at the top of the channel fill differ from those below the channel body in the prominence of drab root traces, suggesting that shallow water tables during final filling promoted the growth of vegetation.

Collectively, these points appear to suggest a relatively humid, seasonal climate during the deposition of Channel Body 1. However, the evidence is difficult to assess because it was derived from an abandoned channel where water would have ponded against relatively impermeable paleosols (Marren and Woods 2011). Additionally, modern channels commonly exchange water with adjoining aquifers and riparian zones, receiving subsurface water by hyporheic flow during dry seasons, which influences habitat diversity and ecological processes. Cendón et al. (2010) provided evidence of such an interchange on distal river plains in Australia. At Quaternary archeological sites in Tanzania (Driese and Ashley 2015), local springs increased soil moisture, which promoted vegetation growth and enhanced pedogenic processes, resulting in an elevated estimate of mean annual precipitation in comparison with regional estimates based on other proxies. Although this spring-fed example does not accord with the context of the study site, the Tanzanian example illustrates that local water sources, such as might be derived from periodic floods or shallow aquifers, can modify soils considerably.

For Channel Body 2, thick coarse sediments with high-flow-strength bedforms, waning-flow cycles, and rapid aggradation indicate large volumes of available water and strongly seasonal flow patterns. Although this suggests a more humid climate and a change in flood patterns (Tooth 2000), the channel body may represent a trunk channel within the drainage system, and the change in paleoflow direction suggests a different source area.

In summary, the most robust evidence for paleoclimate at the Colwell Creek Pond site comes from the floodplain soils below Channel Body 1, which suggest a relatively arid, strongly seasonal paleoclimate. In Channel Body 1, pedogenic processes were probably enhanced by local water availability, allowing riparian vegetation to take advantage of a water-dependent habitat (DiMichele et al. 2006). However, a more humid climate during this period cannot be ruled out, and Quaternary climatic and fluvial records document fluctuations over centuries to a few millennia that radically changed water and sediment budgets (Knox 1993; Gibling et al. 2005; Zhang et al. 2009; Ge et al. 2013). Additionally, the later Kungurian was marked by glaciation in Gondwana (Montañez et al. 2007; Fielding et al. 2008) and, although the level of biostratigraphic precision for the Clear Fork Formation precludes detailed correlation, the Colwell Creek Pond strata may have experienced the far-field effects of global climatic changes.

Taphonomy and Preservation of Plant Material

Plant material is commonly preserved as "three-dimensional goethite petrifactions" in the laminated mudstone (Looy 2013), where early mineralization preserved undistorted anatomical structures of stems and leaves (Fig. 11). The absence of cellular crushing or compaction prior to permineralization indicates early infiltration and hardening of iron compounds in the plant tissues (Dunn et al. 1997). In most modern leaves, the hydrophobic waxy cuticle prevents direct reaction with metals (Kok and Van Der Velde 1994; Dunn et al. 1997). However, leaves coated with bacterial biofilms bond readily with Fe^{3+} within minutes of being placed in water that contains $FeCl_3$, whereas those that lack biofilms do not (Dunn et al. 1997; see also Spicer 1977). Additionally, in environments where oxygen and uncomplexed Fe^{3+} are readily accessible, iron bacteria such as *Sphaerotilus* and *Leptothrix* promote iron encrustation on the

leaves (Caldwell and Caldwell 1980; Lütters and Hanert 1989). Bacterially induced iron deposits are present on biological and sediment surfaces in channels of the Amazon Basin (Konhauser et al. 1993). This process may be a viable mechanism for explaining the well-preserved plant remains at the Colwell Creek Pond site.

Some plant parts, especially of conifers, were coated with a layer of goethite that obscured their features. No cellular structure was associated with these coatings. We hypothesize that these layers were originally algal or bacterial films on the surfaces of plants floating in the water or on the bottom. Yellow goethite-rich laminae may indicate the presence of biofilms in the channel, although they lack microbial textures. The lack of destructive bioturbation would have assisted in preserving these remarkable plant fossils.

CONCLUSIONS

The Colwell Creek Pond site of the Clear Fork Formation represents a small abandoned channel or oxbow lake, with standing water and associated relatively high soil moisture in an otherwise generally dry Early Permian landscape. The 5-m-deep channel was abandoned soon after incision and was infilled with laminated and massive terrigenous mudstone, with a low organic content and no indication of carbonate or evaporite minerals. The laminae were laid down by gentle flows in a standing body of water where the impermeable nature of the underlying soils and perhaps exchange with associated aquifers helped to retain water in the abandoned channel. Abundant large plant remains include branch systems of walchian conifers, leaves of *Taeniopteris* and *Auritifolia*, and other seed plants that probably grew in the riparian zone and were blown or washed into the channel.

Due to the absence of bioturbation and roots, sediment laminae in the abandoned channel were well preserved. A combination of low productivity, high sedimentation rate, elevated salinity, and limited bottom- or pore-water oxygenation may have inhibited benthic organisms, but freshwater ecosystems were underpopulated by infauna during the Early Permian, a reflection of an evolutionary delay in colonization of such habitats.

Paleosols in underlying floodplain deposits are interpreted as paleo-Vertisols formed under relatively arid conditions, with evidence for a strongly seasonal and probably evaporative setting. In contrast, paleosols in the upper part of the channel body yield evidence for wetter conditions. Although we cannot rule out a more humid climate for the plant-bearing laminae, the most parsimonious explanation is that the abandoned channel is a site where water was available for plant growth and preservation in an otherwise relatively arid plain. The exceptional preservation of plant material is attributed to early biomineralization and rapid burial in the absence of burrowing organisms.

ACKNOWLEDGMENTS

We thank A.B. Wharton and G. Willingham of the W.T. Waggoner Estate, Vernon, Texas, for property access to the Colwell Creek Pond site. Polished thin sections were prepared at Dalhousie University by Gordon Brown. We thank David Piper, Owen Brown, Lori Campbell, and Jenna Higgins at Bedford Institute of Oceanography for assistance with X-ray diffraction and total-carbon analyses. We thank Georgia Pe-Piper and Xiang Yang at Saint Mary's University for their guidance with the analysis and interpretation of the SEM data. Constructive and helpful reviews of the manuscript were provided by Steven Driese, Anne Raymond, John Southard, and Associate Editors Elizabeth Gierlowski-Kordesch and Gary Weissmann. Research was funded by a Discovery Grant assigned to Martin Gibling from the Natural Sciences and Engineering Research Council of Canada (NSERC) and by various grants from the Smithsonian Institution to W.A. DiMichele.

REFERENCES

Abdullatif, O.M., 1989, Channel-fill and sheet-flood facies sequences in the ephemeral River Gash, Kassala, Sudan: Sedimentary Geology, v. 63, p. 171–184.

Alexander, J., and Fielding, C.R., 1997, Gravel antidunes in the tropical Burdekin River, Queensland, Australia: Sedimentology, v. 44, p. 327–337.

Allen, J.P., Fielding, C.R., Rygel, M.C., and Gibling, M.R., 2013, Deconvolving signals of tectonic and climatic controls from continental basins: an example from the late Paleozoic Cumberland Basin, Atlantic Canada: Journal of Sedimentary Research, v. 83, p. 847–872.

Anderson, R.Y., and Dean, W.E., 1988, Lacustrine varve formation through time: Palaeogeography, Palaeoclimatology, Palaeoecology, v. 62, p. 215–235.

Arakel, A.V., and McConchie, D., 1982, Classification and genesis of calcrete and gypsite lithofacies in paleodrainage systems of inland Australia and their relationship to carnotite mineralization: Journal of Sedimentary Petrology, v. 52, p. 1149–1170.

Aslan, A., and Autin, W.J., 1998, Holocene flood-plain soil formation in the southern lower Mississippi Valley: implications for interpreting alluvial paleosols: Geological Society of America Bulletin, v. 110, p. 433–449.

Bashforth, A.R., Cleal, C.J., Gibling, M.R., Falcon-Lang, H.J., and Miller, R.F., 2014, Paleoecology of early Pennsylvanian vegetation on a seasonally dry tropical landscape (Tynemouth Creek Formation, New Brunswick, Canada): Review of Palaeobotany and Palynology, v. 200, p. 229–263.

Bashforth, A.R., DiMichele, W.A., and Eble, C.F., **in press**, Dryland vegetation from the Middle Pennsylvanian of Indiana (Illinois Basin): the dryland biome in glacioeustatic, paleobiogeographic, and paleoecologic context: Journal of Paleontology.

Batenburg, L.H., 1982, "Compression species" and "petrifaction species" of *Sphenophyllum* compared: Review of Palaeobotany and Palynology, v. 36, p. 335–359.

Bein, A., and Land, L.S., 1983, Carbonate sedimentation and diagenesis associated with Mg-Ca-chloride brines: the Permian San Andres Formation in the Texas Panhandle: Journal of Sedimentary Petrology, v. 53, p. 243–260.

Bercovici, A., Diez, J.B., Broutin, J., Bourquin, S., Linol, B., Villanueva-Amadoz, U., López-Gómez, J., and Durand, M., 2009, A palaeoenvironmental analysis of Permian sediments in Minorca (Balearic Islands, Spain) with new palynological and megafloral data: Review of Palaeobotany and Palynology, v. 158, p. 14–28.

Bradley, W.H., 1931, Origin and microfossils of the oil shale of the Green River Formation of Colorado and Utah: U.S. Geological Survey, Professional Paper 168, p. 28–29.

Brister, B.S., Stephens, W.C., and Norman, G.A., 2002, Structure, stratigraphy and hydrocarbon systems of a Pennsylvanian pull-apart basin in north-central Texas: American Association of Petroleum Geologists, Bulletin, v. 86, p. 1–20.

Brown, L.F., 1973, Pennsylvanian rocks of north-central Texas: an introduction, *in* Brown, J.L.F., ed., Pennsylvanian Depositional Systems in North-Central Texas: A Guide For Interpreting Terrigenous Clastic Facies in a Cratonic Basin: University of Texas at Austin, Bureau of Economic Geology, Guidebook 14, p. 1–9.

Buatois, L.A., and Mángano, M.G., 1993, Ecospace utilization, paleoenvironmental trends, and the evolution of early nonmarine biotas: Geology, v. 21, p. 595–598.

Buatois, L.A., Mángano, M.G., Genise, J.F., and Taylor, T.N., 1998, The ichnologic record of the continental invertebrate invasion: evolutionary trends in environmental expansion, ecospace utilization, and behavioral complexity: Palaios, v. 13, p. 217–240.

Budnik, R.T., 1989, Tectonic Structures of the Palo Duro Basin, Texas Panhandle: University of Texas at Austin, Bureau of Economic Geology, Report of Investigations, v. 187, 43 p.

Burnham, R.J., 1989, Relationships between standing vegetation and leaf litter in a paratropical forest: implications for paleobotany: Review of Palaeobotany and Palynology, v. 58, p. 5–32.

Caldwell, D.E., and Caldwell, S.J., 1980, Fine structure of in situ microbial iron deposits: Geomicrobiology Journal, v. 2, p. 39–53.

Calvo, J.P., Rodriguez-Pascua, M., Martin-Velazquez, S., Jimenez, S., and Vicente, G.D., 1998, Microdeformation of lacustrine laminite sequences from Late Miocene formations of SE Spain: an interpretation of loop bedding: Sedimentology, v. 45, p. 279–292.

Cendón, D.I., Larsen, J.R., Jones, B.G., Nanson, G.C., Rickleman, D., Hankin, S.I., Pueyo, J.J., and Maroulis, J., 2010, Freshwater recharge into a shallow saline groundwater system, Cooper Creek floodplain, Queensland, Australia: Journal of Hydrology, v. 392, p. 150–163.

Chaney, D.S., and DiMichele, W.A., 2007, Paleobotany of the classic redbeds (Clear Fork Formation, Early Permian) of north-central Texas, *in* Wong, T.E., ed., Proceedings of the XVth International Congress on Carboniferous and Permian Stratigraphy, University of Utrecht, the Netherlands, p. 357–366.

Chaney, D.S., Sues, H.D., and DiMichele, W.A., 2005, A juvenile skeleton of the nectridean amphibian *Diplocaulus* and associated flora and fauna from the Mitchell Creek Flats locality (upper Waggoner Ranch Formation; Early Permian), Baylor County, north-central Texas: New Mexico Museum of Natural History and Science, Bulletin, v. 30, p. 39–47.

Chaney, D.S., Mamay, S.H., DiMichele, W.A., and Kerp, H., 2009, *Auritifolia* gen. nov., probable seed plant foliage with comioid affinities from the Early Permian of Texas, U.S.A: International Journal of Plant Sciences, v. 170, p. 247–266.

Clausing, A., and Boy, J.A., 2000, Lamination and primary production in fossil lakes: relationship to palaeoclimate in the Carboniferous–Permian transition, *in* Hart, M.B., ed., Climates: Past and Present: Geological Society of London, Special Publication 181, p. 5–16.

Cohen, A.S., 1984, Effect of zoobenthic standing crop on laminae preservation in tropical lake sediment, Lake Turkana, East Africa: Journal of Paleontology, v. 58, p. 499–510.

Cole, R.D., and Picard, M.D., 1975, Primary and secondary sedimentary structures in oil shale and other fine grained rocks, Green River Formation (Eocene), Utah and Colorado: Utah Geology, v. 2, p. 49–67.

Colson, J., and Cojan, I., 1996, Groundwater dolocretes in a lake-marginal environment: an alternative model for dolocrete formation in continental settings (Danian of the Provence Basin, France): Sedimentology, v. 43, p. 175–188.

de Gibert, J.M., and Ekdale, A.A., 2002, Ichnology of a restricted epicontinental sea, Arapien Shale, Middle Jurassic, Utah, USA: Palaeogeography, Palaeoclimatology, Palaeoecology, v. 183, p. 275–286.

Dean, W.E., and Fouch, T.D., 1983, Lacustrine Environment, *in* Scholle, P.A., Bebout, D.G., and Moore, G.H., eds., Carbonate Depositional Environments: American Association of Petroleum Geologist, Memoir 33, p. 97–130.

Demicco, R.V., and Gierlowski-Kordesch, E.G., 1986, Facies sequences of a semi-arid closed basin: the Lower Jurassic East Berlin Formation of the Hartford Basin, New England, USA: Sedimentology, v. 33, p. 107–118.

Demko, T.M., 1995, Taphonomy of fossil plants in the Upper Triassic Chinle Formation [Unpublished Ph.D. dissertation]: University of Arizona, Tucson, 274 p.

DiMichele, W.A., and Aronson, R.B., 1992, The Pennsylvanian–Permian vegetational transition: a terrestrial analogue to the Onshore–Offshore Hypothesis: Evolution, v. 46, p. 807–824.

DiMichele, W.A., Kerp, H., Krings, M., and Chaney, D.S., 2005, The Permian peltasperm radiation: evidence from the southwestern United States: New Mexico Museum of Natural History and Science, Bulletin, v. 30, p. 67–79.

DiMichele, W.A., Tabor, N.J., Chaney, D.S., and Nelson, W.J., 2006, From wetlands to wet spots: environmental tracking and the fate of Carboniferous elements in Early Permian tropical floras, *in* Greb, S.F., and DiMichele, W.A., eds., Wetlands through Time: Geological Society of America, Special Paper 399, p. 223–248.

DiMichele, W.A., Cecil, C.B., Chaney, D.S., Elrick, S.D., and Nelson, W.J., 2014, Fossil floras from the Pennsylvanian–Permian Cutler Group of southeastern Utah: Utah Geological Association, Publication 43, p. 491–504.

Donovan, R.N., and Foster, R.J., 1972, Subaqueous shrinkage cracks from Caithness Flagstone Series (middle Devonian) of northeast Scotland: Journal of Sedimentary Petrology, v. 42, p. 309–317.

Driese, S.G., and Ashley, G.M., 2015, Paleoenvironmental reconstruction of a paleosol catena, the Zinj archeological level, Olduvai Gorge, Tanzania: Quaternary Research, v. 85, p. 133–146

Dunn, K.A., McLean, R.J., Upchurch, G.R., and Folk, R.L., 1997, Enhancement of leaf fossilization potential by bacterial biofilms: Geology, v. 25, p. 1119–1122.

Edwards, M.B., Eriksson, K.A., and Kier, R.S., 1983, Paleochannel geometry and flow patterns determined from exhumed Permian point bars in north-central Texas: Journal of Sedimentary Petrology, v. 53, p. 1261–1270.

Falcon-Lang, H.J., and Bashforth, A.R., 2005, Morphology, anatomy, and upland ecology of large cordaitalean trees from the middle Pennsylvanian of Newfoundland: Review of Palaeobotany and Palynology, v. 135, p. 223–243.

Fielding, C.R., 2006, Upper flow regime sheets, lenses and scour fills: extending the range of architectural elements for fluvial sediment bodies: Sedimentary Geology, v. 190, p. 227–240.

Fielding, C.R., Frank, T.D., Birgenheier, L.P., Rygel, M.C., Jones, A.T., and Roberts, J., 2008, Stratigraphic imprint of the late Palaeozoic Ice Age in eastern Australia: a record of alternating glacial and nonglacial climate regime: Geological Society of London, Journal, v. 165, p. 129–140.

Florin, R., 1954, The female reproductive organs of conifers and taxads: Biological Reviews, v. 29, p. 367–389.

Fregenal-Martinez, M.A., and Melendez, N., 1994, Sedimentological analysis of the Lower Cretaceous lithographic limestones of the "Las Hoyas" fossil site (Serrania de Cuenca, Iberian Range, Spain): Geobios, v. 27, p. 185–193.

Galtier, J., and Broutin, J., 2008, Floras from red beds of the Permian Basin of Lodève (Southern France): Journal of Iberian Geology, v. 34, p. 57–72

Gastaldo, R.A., 1989, Preliminary observations on phytotaphonomic assemblages in a subtropical/temperate Holocene bayhead delta: Mobile Delta, Gulf Coastal Plain, Alabama: Review of Palaeobotany and Palynology, v. 58, p. 61–83.

Ge, Q., Hao, Z., Zheng, J., and Shao, X., 2013, Temperature changes over the past 2000 yr in China and comparison with the Northern Hemisphere: Climate of the Past, v. 9, p. 1153–1160.

Gevers, T.W., Frakes, L.A., Edwards, L.N., and Marzolf, J.E., 1971, Trace fossils from the Lower Beacon sediments (Devonian), Darwin Mountains, southern Victoria Land, Antarctica: Journal of Paleontology, v. 45, p. 81–94.

Gibling, M.R., 2006, Width and thickness of fluvial channel bodies and valley fills in the geological record: a literature compilation and classification: Journal of Sedimentary Research, v. 76, p. 731–770.

Gibling, M.R., Tantisukrit, C., Uttamo, W., Thanasuthipitak, T., and Haraluck, M., 1985, Oil shale sedimentology and geochemistry in Cenozoic Mae Sot basin, Thailand: American Association of Petroleum Geologists, Bulletin, v. 69, p. 767–780.

Gibling, M.R., Nanson, G.G., and Maroulis, J.C., 1998, Anastomosing river sedimentation in the Channel Country of central Australia: Sedimentology, v. 45, p. 595–619.

Gibling, M.R., Tandon, S.K., Sinha, R., and Jain, M., 2005, Discontinuity-bounded alluvial sequences of the southern Gangetic Plains, India: aggradation and degradation in response to monsoonal strength: Journal of Sedimentary Research, v. 75, p. 369–385.

Gilbert, M.C., 1982, Geology of the Eastern Wichita Mountains, with a brief discussion of unresolved problems, *in* Gilbert, M.C., and Donovan, R.N., eds., Geology of the Eastern Wichita Mountains, Southwestern Oklahoma: Oklahoma Geological Survey, Guidebook 21, p. 1–28.

Guccione, M.J., 1993, Grain-size distribution of overbank sediment and its use to locate channel positions, *in* Marzo, M., and Puigdefabregas, C., eds., Alluvial Sedimentation: International Association of Sedimentologists, Special Publication 17, p. 185–194.

Guccione, M.J., Burford, M.F., and Kendall, J.D., 1999, Pemiscot Bayou, a large distributary of the Mississippi River and a possible failed avulsion, *in* Smith, N.D., and Rogers, J., eds., Fluvial Sedimentology VI: International Association of Sedimentologists, Special Publication 28, p. 211–220.

Hackley, P.C., Guevara, E.H., Hentz, T.F., and Hook, R.W., 2009, Thermal maturity and organic composition of Pennsylvanian coals and carbonaceous shales, north-central Texas: implications for coalbed gas potential: International Journal of Coal Geology, v. 77, p. 294–309.

Ham, W.E., 1973, Regional geology of the Arbuckle Mountains, Oklahoma: Oklahoma Geological Survey, Special Publication 73, p. 1–55.

Hartley, A.J., Weissmann, G.S., Bhattacharayya, P., Nichols, G.J., Scuderi, L.A., Davidson, S.K., Leleu, S., Chakraborty, T., Ghosh, P., and Mather, A.E., 2013, Soil development on modern distributive fluvial systems: preliminary observations with implications for interpretation of paleosols in the rock record, *in* Driese, S., ed., New Frontiers in Paleopedology and Terrestrial Paleoclimatology: SEPM, Special Publication 104, p. 149–158.

Hentz, T.F., 1988, Lithostratigraphy and paleoenvironments of Upper Paleozoic continental red beds, North-Central Texas: Bowie (new) and Wichita (revised) Groups: University of Texas at Austin, Bureau of Economic Geology, Report of Investigations, v. 170, p. 47–55.

Hesselbo, S.P., and Trewin, N.H., 1984, Deposition, diagenesis and structures of the Cheese Bay Shrimp Bed, Lower Carboniferous, East Lothian: Scottish Journal of Geology, v. 20, p. 281–296.

Hotton, N., III, Feldmann, R.M., Hook, R.W., and DiMichele, W.A., 2002, Crustacean-bearing continental deposits in the Petrolia Formation (Leonardian Series, Lower Permian) of north-central Texas: Journal of Paleontology, v. 76, p. 486–494.

Johnson, G.D., 2012, Possible origin of the xenacanth sharks *Orthacanthus texensis* and *Orthacanthus platypternus* in the Lower Permian of Texas, USA: Historical Biology, v. 24, p. 369–379.

Kelts, K., and Hsü, K.J., 1978, Freshwater carbonate sedimentation, *in* Lerman, A., ed., Lakes: New York, Springer, p. 295–323.

Kerp, J.H., 1988, Aspects of Permian palaeobotany and palynology. X. The West and Central European species of the genus *Autunia* Krasser emend. Kerp (Peltaspermaceae) and the form-genus *Rhachiphyllum* Kerp (callipterid foliage): Review of Palaeobotany and Palynology, v. 54, p. 249–360.

Kessler, J.L., Soreghan, G.S., and Wacker, H.J., 2001, Equatorial aridity in western Pangea: Lower Permian loessite and dolomitic paleosols in northeastern New Mexico, USA: Journal of Sedimentary Research, v. 71, p. 817–832.

Kinne, O., 1970, 4. Salinity, 4.3. Animals, 4.3.1. Invertebrates, *in* Kinne, O., ed., Marine Ecology: A Comprehensive, Integrated Treatise of Life in Oceans and Coastal Waters: New York, Wiley-Interscience, p. 821–996.

Knighton, A.D., and Nanson, G.C., 1993, Anastomosis and the continuum of the channel pattern: Earth Surface Processes and Landforms, v. 18, p. 613–625.

Knighton, A.D., and Nanson, G.C., 1994a, Flow transmission along an arid zone anastomosing river, Cooper Creek, Australia: Hydrological Processes, v. 8, p. 137–154.

Knighton, A.D., and Nanson, G.C., 1994b, Waterholes and their significance in the anastomosing channel system of Cooper Creek, Australia: Geomorphology, v. 9, p. 311–324.

Knox, J.C., 1993, Large increases in flood magnitude in response to modest changes in climate: Nature, v. 361, p. 430–432.

Kok, C.J., and Van Der Velde, G., 1994, Decomposition and macroinvertebrate colonization of aquatic and terrestrial leaf material in alkaline and acid still water: Freshwater Biology, v. 31, p. 65–75.

Konhauser, K.O., Fyfe, W.S., Ferris, F.G., and Beveridge, T.J., 1993, Metal sorption and mineral precipitation by bacteria in two Amazonian river systems: Rio Solimões and Rio Negro, Brazil: Geology, v. 21, p. 1103–1106.

Krings, M., Klavins, S.D., DiMichele, W.A., Kerp, H., and Taylor, T.N., 2005, Epidermal anatomy of *Glenopteris splendens* Sellards nov. emend., an enigmatic seed plant from the Lower Permian of Kansas (USA): Review of Palaeobotany and Palynology, v. 136, p. 159–180.

Labandeira, C.C., and Allen, E.G., 2007, Minimal insect herbivory for the Lower Permian Coprolite Bone Bed site of north-central Texas, USA, and comparison to other Late Paleozoic floras: Palaeogeography, Palaeoclimatology, Palaeoecology, v. 247, p. 197–219.

Langford, R., and Bracken, B., 1987, Medano Creek, Colorado, a model for upper-flow-regime fluvial deposition: Journal of Sedimentary Petrology, v. 57, p. 863–870.

Laveine, J.-P., and Dufour, F., 2013, The bifurcate "outer–inner" semi-pinnate frond of the Permo-Pennsylvanian seed-fern *Neurodontopteris auriculata*, type species of the genus *Neurodontopteris*: Palaeontographica, v. 289B, p. 75–177.

Li, H., and Taylor, D.W., 1998, *Aculeovinea yunguiensis* gen. et sp. nov., a new taxon of gigantopterid axis from the Upper Permian of Guizhou province, China: International Journal of Plant Science, v. 159, p. 1023–1033.

Li, H., and Taylor, D.W., 1999, Vessel-bearing stems of *Vasovinea tianii* gen. et sp. nov. (Gigantopteridales) from the Upper Permian of Guizhou province, China: American Journal of Botany, v. 86, p. 1563–1575.

Lojka, R., Drábková, J., Zajíc, J., Sýkorová, I., Franců, J., Bláhová, A., and Grygar, T., 2009, Climate variability in the Stephanian B based on environmental record of the Mšec Lake deposits (Kladno–Rakovník Basin, Czech Republic): Palaeogeography, Palaeoclimatoloty, Palaeoecology, v. 280, p. 78–93.

Long, G.F., 2011, Architecture and depositional style of fluvial systems before land plants: a comparison of Precambrian, Early Paleozoic, and modern river deposits, *in* North, C.P., Davidson, S., and Leleu, S., eds., From River to Rock Record: The Preservation of Fluvial Sediments and their Subsequent Interpretation: SEPM, Special Publication 97, p. 37–61.

Looy, C.V., 2013, Natural history of a plant trait: branch-system abscission in Paleozoic conifers and its environmental, autecological, and ecosystem implications in a fire-prone world: Paleobiology, v. 39, p. 235–252.

Looy, C.V., and Duijnstee, I.A., 2013, Characterizing morphologic variability in foliated Paleozoic conifer branches: a first step in testing its potential as proxy for taxonomic composition: New Mexico Museum of Natural History and Science, Bulletin 60, p. 215–223.

Lucas, S.G., Voigt, S., Lerner, A.J., and Nelson, W.J., 2011, Late Early Permian continental ichnofauna from Lake Kemp, north-central Texas, USA: Palaeogeography, Palaeoclimatology, Palaeoecology, v. 308, p. 395–404.

Ludlam, S.D., 1981, Sedimentation rates in Fayetteville Green Lake, New York, USA: Sedimentology, v. 28, p. 85–96.

Lütters, S., and Hanert, H.H., 1989, The ultrastructure of chemolithoautotrophic *Gallionella ferruginea* and *Thiobacillus ferrooxidans* as revealed by chemical fixation and freeze-etching: Archives of Microbiology, v. 151, p. 245–251.

Mamay, S.H., 1989, *Evolsonia*, a new genus of Gigantopteridaceae from the Lower Permian Vale Formation, north-central Texas: American Journal of Botany, v. 76, p. 1299–1311.

Mamay, S.H., Chaney, D.S., and DiMichele, W.A., 2009, *Comia*, a seed plant possibly of peltaspermous affinity: a brief review of the genus and description of two new species from the Early Permian (Artinskian) of Texas, *C. greggii* sp. nov. and *C. craddockii* sp. nov: International Journal of Plant Sciences, v. 170, p. 267–282.

Marren, P.M., and Woods, K.L., 2011, Inundation of anabranching river flood plain wetlands: the Ovens River, Victoria, Australia, *in* Abesser, C., Nützmann, G., Hill, M.C., Blöschl, G., and Lakshmanan, E., eds., Conceptual and Modelling Studies of Integrated Groundwater, Surface Water and Ecological Systems: International Association of Hydrological Sciences, Publication 345, p. 229–234.

McCaffrey, M.A., Lazar, B., and Holland, H.D., 1987, The evaporation path of seawater and the coprecipitation of Br^- and K^+ with halite: Journal of Sedimentary Petrology, v. 57, p. 928–937.

Menounos, B., Clague, J., Gilbert, R., and Slaymaker, O., 2005, Environmental reconstruction from a varve network in the southern Coast Mountains, British Columbia, Canada: The Holocene, v. 15, p. 1163–1171.

Mertes, L.A., 1997, Documentation and significance of the perirheic zone on inundated floodplains: Water Resources Research, v. 33, p. 1749–1762.

Miall, A.D., 1985, Architectural-element analysis: a new method of facies analysis applied to fluvial deposits: Earth-Science Reviews, v. 22, p. 261–308.

Miall, A.D., 1996, The Geology of Fluvial Deposits: Sedimentary Facies, Basin Analysis and Petroleum Geology: Berlin, Springer-Verlag, 582 p.

Miller, J.R., 1991, Development of anastomosing channels in south-central Indiana: Geomorphology, v. 4, p. 221–229.

Miller, M.F., 1984, Distribution of biogenic structures in Paleozoic nonmarine and marine-margin sequences: an actualistic model: Journal of Paleontology, v. 58, p. 550–570.

Miller, M.F., and Labandeira, C.C., 2002, The slow crawl across the salinity divide: delayed colonization of freshwater ecosystems by invertebrates: GSA Today, v. 12, p. 4–10.

Minter, N.J., Krainer, K., Lucas, S.G., Braddy, S.J., and Hunt, A.P., 2007, Palaeoecology of an Early Permian playa lake trace fossil assemblage from Castle Peak, Texas, USA: Palaeogeography, Palaeoclimatology, Palaeoecology, v. 246, p. 390–423.

Mohrig, D., Heller, P.L., Paola, C., and Lyons, W.J., 2000, Interpreting avulsion process from ancient alluvial sequences: Guadalope–Matarranya system (northern Spain) and Wasatch Formation (western Colorado): Geological Society of America, Bulletin 112, p. 1787–1803.

Montañez, I.P., Tabor, N.J., Niemeier, D., DiMichele, W.A., Frank, T.D., Fielding, C.R., Isbell, J.L., Birgenheier, L.P., and Rygel, M.C., 2007, CO_2-forced climate and vegetation instability during late Paleozoic deglaciation: Science, v. 315, p. 87–91.

Moore, D.M., and Reynolds, R.C., 1997, X-ray Diffraction and the Identification and Analysis of Clay Minerals: Oxford, Oxford University Press, 378 p.

Morozova, G.S., and Smith, N.D., 2000, Holocene avulsion styles and sedimentation patterns of the Saskatchewan River, Cumberland Marshes, Canada: Sedimentary Geology, v. 130, p. 81–105.

Munsell Color, 1994, Munsell Soil Color Charts (revised edition): New Windsor, New York, Munsell Color, 10 p.

Murry, P.A., and Johnson, G.D., 1987, Clear Fork vertebrates and environments from the Lower Permian of north-central Texas: Texas Journal of Science, v. 39, p. 253–266.

Naugolnykh, S.V., 1999, A new species of *Compsopteris* Zalessky from the Upper Permian of the Kama River Basin (Perm Region): Paleontological Journal, v. 33, p. 686–697.

Nelson, W.J., Hook, R.W., and Chaney, D.S., 2013, Lithostratigraphy of the Lower Permian (Leonardian) Clear Fork Formation of north-central Texas, *in* Lucas, S.G., DiMichele, W.A., Barrick, J.E., Schneider, J.W., and Spielmann, J.A., eds., The Carboniferous–Permian transition: New Mexico Museum of Natural History and Science, Bulletin 60, p. 286–311.

Netto, R.G., Balistieri, P.R.M.N., Lavina, E.L.C., and Silveira, D.M., 2009, Ichnological signatures of shallow freshwater lakes in the glacial Itararé Group (Mafra Formation, Upper Carboniferous–Lower Permian of Paraná Basin, S Brazil): Palaeogeography, Palaeoclimatology, Palaeoecology, v. 272, p. 240–255.

Olson, E.C., 1958, Fauna of the Vale and Choza: Fieldiana Geology, v. 10, p. 397–448.

Olson, E.C., 1989, The Arroyo Formation (Leonardian: Lower Permian) and its vertebrate fossils: Texas Memorial Museum, Bulletin 35, 25 p.

Olson, E.C., and Bolles, K., 1975, Permo-Carboniferous fresh water burrows: Fieldiana, Geology, v. 33, p. 271–290.

Olson, E.C., and Mead, J.G., 1982, The Vale Formation (Lower Permian), its vertebrates and paleoecology: Texas Memorial Museum, Bulletin 29, 46 p.

Petersen, G.W., Chester, G., and Lee, G.B., 1966, Quantitative determination of calcite and dolomite in soils: Journal of Soil Science, v. 17, p. 328–338.

Pittermann, J., Stuart, S.A., Dawson T.E., and Moreau, A., 2012, Cenozoic climate change shaped the evolutionary ecophysiology of the Cupressaceae conifers: National Academy of Sciences (USA), Proceedings, v. 109, p. 9647–9652.

Pokorný, P., Klimešová, J., and Klimeš, L., 2000, Late Holocene history and vegetation dynamics of a floodplain alder carr: a case study from eastern Bohemia, Czech Republic: Folia Geobotanica, v. 35, p. 43–58.

Prevec, R., Labandeira, C.C., Neveling, J., Gastaldo, R.A., Looy, C.V., and Bamford, M., 2009, Portrait of a Gondwanan ecosystem: a new late Permian fossil locality from KwaZulu–Natal, South Africa: Review of Palaeobotany and Palynology, v. 156, p. 454–493.

Price, A.R., 1982, Western Arabian Gulf echinoderms in high salinity waters and the occurrence of dwarfism: Journal of Natural History, v. 16, p. 519–527.

Raymond, A., Lambert, L., Costanza, S., Slone, E.J., and Cutlip, P.C., 2010, Cordaiteans in paleotropical wetlands: an ecological re-evaluation: International Journal of Coal Geology, v. 83, p. 248–265.

Rees, P.M., Ziegler, A.M., Gibbs, M.T., Kutzbach, J.E., Behling, P.J., and Rowley, D.B., 2002, Permian phytogeographic patterns and climate data/model comparisons: Journal of Geology, v. 110, p. 1–3.

Regan, T.R., and Murphy, P.J., 1986a, Faulting in the Matador Uplift area, Texas: Stone and Webster Engineering, Boston, Topical Report ONWI/SUB/86/E512-05000-T48, 169 p.

Remy, W., and Remy, R., 1975, Beiträge zur Kenntnis des Morpho-Genus *Taeniopteris* Brongniart: Argumenta Palaeobotanica, v. 4, p. 31–37.

Rothwell, G.W., 1982, New interpretations of the earliest conifers: Review of Palaeobotany and Palynology, v. 37, p. 7–28.

Rowland, J.C., Lepper, K., Dietrich, W.E., Wilson, C.J., and Sheldon, R., 2005, Tie channel sedimentation rates, oxbow formation age and channel migration rate from optically stimulated luminescence (OSL) analysis of floodplain deposits: Earth Surface Processes and Landforms, v. 30, p. 1161–1179.

Sander, P.M., 1987, Taphonomy of the Lower Permian Geraldine bonebed in Archer County, Texas: Palaeogeography, Palaeoclimatology, Palaeoecology, v. 61, p. 221–236.

Schachat, S., Labandeira, C.C., Gordon, J., Chaney, D., Levi, S., Halthore, M.S., and Alvarez, J., 2014, Plant–insect interactions from the Early Permian (Kungurian) Colwell Creek Pond, North-Central Texas: the early spread of herbivory in riparian environments: International Journal of Plant Sciences, v. 175, p. 855–890.

Scheihing, M.H., 1980, Reduction of wind velocity by the forest canopy and the rarity of non-arborescent plants in the Upper Carboniferous fossil record: Argumenta Palaeobotanica, v. 6, p. 133–138.

Scheihing, M.H., and Pfefferkorn, H.W., 1984, The taphonomy of land plants in the Orinoco Delta: a model for the incorporation of plant parts in clastic sediments of Late Carboniferous age of Euramerica: Review of Palaeobotany and Palynology, v. 41, p. 205–240.

Schmid, S., Worden, R.H., and Fisher, Q.J., 2006, Sedimentary facies and the context of dolocrete in the Lower Triassic Sherwood Sandstone group: Corrib Field west of Ireland: Sedimentary Geology, v. 187, p. 205–227.

Shanahan, T.M., Overpeck, J.T., Beck, J.W., Wheeler, C.W., Peck, J.A., King, J.W., and Scholz, C.A., 2008, The formation of biogeochemical laminations in Lake Bosumtwi, Ghana, and their usefulness as indicators of past environmental changes: Journal of Paleolimnology, v. 40, p. 339–355.

Sharma, S., Joachimski, M., Sharma, M., Tobschall, H.J., Singh, I.B., Sharma, C., Chauhan, M.S., and Morgenroth, G., 2004, Late glacial and Holocene environmental changes in Ganga plain, Northern India: Quaternary Science Reviews, v. 23, p. 145–159.

Slingerland, R., and Smith, N.D., 2004, River avulsions and their deposits: Annual Review of Earth and Planetary Sciences, v. 32, p. 257–285.

Smith, N.D., Morozova, G.S., and Gibling, M.R., 2014, Channel enlargement by avulsion-induced sediment starvation in the Saskatchewan River: Geology, v. 42, p. 355–358.

Spicer, R.A., 1977, The pre-dispositional formation of some leaf impressions: Palaeontology, v. 20, p. 907–912.

Spötl, C., and Wright, V.P., 1992, Groundwater dolocretes from the Upper Triassic of the Paris Basin, France: a case study of an arid, continental diagenetic facies: Sedimentology, v. 39, p. 1119–1136.

Sugden, W., 1963, The hydrology of the Persian Gulf and its significance in respect to evaporite deposition: American Journal of Science, v. 261, p. 741–755.

Tabor, N.J., 2013, Wastelands of tropical Pangea: high heat in the Permian: Geology, v. 4, p. 623–624.

Tabor, N.J., and Montañez, I.P., 2004, Morphology and distribution of fossil soils in the Permo-Pennsylvanian Wichita and Bowie groups, north-central Texas, USA: Implications for western equatorial Pangean palaeoclimate during icehouse–greenhouse transition: Sedimentology, v. 51, p. 851–884.

Tabor, N.J., and Poulsen, C.J., 2008, Palaeoclimate across the Late Pennsylvanian–Early Permian tropical palaeolatitudes: a review of climate indicators, their distribution, and relation to palaeophysiographic climate factors: Palaeogeography, Palaeoclimatology, Palaeoecology, v. 268, p. 293–310.

Tabor, N.J., Romanchock, C.M., Looy, C.V., Hotton, C.L., DiMichele, W.A., and Chaney, D.S., 2013, Conservatism of Late Pennsylvanian vegetational patterns during short-term cyclic and long-term directional environmental change, western equatorial Pangea: Geological Society of London, Special Publication 376, p. 201–234.

Toonen, W.H.J., Kleinhans, M.G., and Cohen, K.M., 2012, Sedimentary architecture of abandoned channel fills: Earth Surface Processes and Landforms, v. 37, p. 459–472.

Tooth, S., 2000, Process, form and change in dryland rivers: a review of recent research: Earth-Science Reviews, v. 51, p. 67–107.

Trewin, N.H., 1986, Palaeoecology and sedimentology of the Achanarras fish bed of the Middle Old Red Sandstone, Scotland: Royal Society of Edinburgh, Transactions, Earth Sciences, v. 77, p. 21–46.

Tucker, M.E., 2003, Sedimentary Rocks in the Field: Chichester, U.K., John Wiley, 234 p.

Verschuren, D., 1999, Sedimentation controls on the preservation and time resolution of climate-proxy records from shallow fluctuating lakes: Quaternary Science Reviews, v. 18, p. 821–837.

Wan, M., and Wang, J., 2015, *Nanshanopteris nervosa* gen. et sp. nov., a glenopterid foliage from the Changhsingian Sunan Formation in Yumen, western China: Review of Palaeobotany and Palynology, v. 219, p. 39–51.

Weissmann, G.S., Hartley, A.J., Scuderi, L.A., Nichols, G.J., Davidson, S.K., Owen, A., Atchley, S.C., Bhattacharyya, P., Chakraborty, T., Ghosh, P., and Nordt, L.C., 2013, Prograding distributive fluvial systems: geomorphic models and ancient examples, *in* Driese, S.G., and Nordt, L.C., eds., New Frontiers in Paleopedology and Terrestrial Paleoclimatology: SEPM, Special Publication 104, p. 131–147.

Weissmann, G.S., Hartley, A.J., Scuderi, L.A., Nichols, G.J., Owen, A., Wright, S., Felicia, A.L., Holland, F., and Anaya, F.M.L., 2015, Fluvial geomorphic elements in modern sedimentary basins and their potential preservation in the rock record: a review: Geomorphology, v. 250, p. 187–219.

White, D., 1929, Flora of the Hermit Shale, Grand Canyon, Arizona: Carnegie Institution of Washington, Publication 405, 221 p.

Wilson, M.V., 1977, Paleoecology of Eocene lacustrine varves at Horsefly, British Columbia: Canadian Journal of Earth Sciences, v. 14, p. 953–962.

Wren, D.G., Davidson, G.R., Walker, W.G., and Galicki, S.J., 2008, The evolution of an oxbow lake in the Mississippi alluvial floodplain: Journal of Soil and Water Conservation, v. 63, p. 129–135.

Wright, I.J., Reich, P.B., Westoby, M., Ackerly, D.D., Baruch, Z., Bongers, F., Cavender-Bares, J., Chapin, T., Cornelissen, J.H.C., Diemer, M., Flexas, J., Garnier, E., Groom, P.K., Gulias, J., Hikosaka, K., Lamont, B.B., Lee, T., Lee, W., Lusk, C., Midgley, J.J., Navas, M.-L., Niinemets, Ü., Oleksyn, J., Osada, N., Poorter, H., Poot, P., Prior, L., Pyankov, V.I., Roumet, C., Thomas, S.C., Tjoelker, M.G., Veneklaas, E.J., and Villar, R., 2004, The worldwide leaf economics spectrum: Nature, v. 428, p. 821–827.

Zaleha, M.J., 1997a, Fluvial and lacustrine palaeoenvironments of the Miocene Siwalik Group, Khaur area, northern Pakistan: Sedimentology, v. 44, p. 349–368.

Zaleha, M.J., 1997b, Intra- and extra-basinal controls on fluvial deposition in the Miocene Indo-Gangetic foreland basin, northern Pakistan: Sedimentology, v. 44, p. 369–390.

Zambito, J.J., and Benison, K.C., 2013, Extremely high temperatures and paleoclimate trends recorded in Permian ephemeral lake halite: Geology, v. 41, p. 587–590.

Zhang, Z., Gong, D., He, X., Guo, D., and Feng, S., 2009, Reconstruction of the western Pacific warm pool SST since 1644 AD and its relation to precipitation over East China: Science in China, Series D, Earth Sciences, v. 52, p. 1436–1446.

Ziegler, A.M., Hulver, M.L., and Rowley, D.B., 1997, Permian world topography and climate, *in* Martini, I., ed., Late Glacial and Postglacial Environmental Changes: Pleistocene, Carboniferous–Permian, and Proterozoic: Oxford, UK, Oxford University Press, p. 111–146.

Received 25 November 2015; accepted 2 June 2016.